

Classification of robust isolated vortices in two-dimensional hydrodynamics

By P. H. CHAVANIS AND J. SOMMERIA

Ecole Normale Supérieure de Lyon, 69364 Lyon cedex 07, France

(Received 2 August 1996 and in revised form 12 September 1997)

We determine solutions of the Euler equation representing isolated vortices (monopoles, dipoles) in an infinite domain, for arbitrary values of energy, circulation, angular momentum and impulse. A linear relationship between vorticity and stream function is assumed inside the vortex (while the flow is irrotational outside). The emergence of these solutions in a turbulent flow is justified by the statistical mechanics of continuous vorticity fields. The additional restriction of mixing to a ‘maximum-entropy bubble’, due to kinetic constraints, is assumed. The linear relationship between vorticity and stream function is obtained from the statistical theory in the limit of strong mixing (when constraints are weak). In this limit, maximizing entropy becomes equivalent to a kind of enstrophy minimization. New stability criteria are investigated and imply in particular that, in most cases, the vorticity must be continuous (or slightly discontinuous) at the vortex boundary. Then, the vortex radius is automatically determined by the integral constraints and we can obtain a classification of isolated vortices such as monopoles and dipoles (rotating or translating) in terms of a single control parameter. This article generalizes the classification obtained in a bounded domain by Chavanis & Sommeria (1996).

1. Introduction

The formation of organized vortices is an intriguing phenomenon in two-dimensional turbulence. It has been observed in many numerical simulations of two-dimensional turbulence, as first emphasized and investigated by McWilliams (1984). It is also observed in laboratory experiments (Flierl, Stern & Whitehead 1983; Couder & Basdevant 1986; Nguyen duc & Sommeria 1988; van Heijst & Flor 1989) and in the atmospheres or oceans (see e.g. Stern 1975; Flierl 1987). Different structures have been observed, which can be classified as axisymmetric monopoles and rotating or translating dipoles (involving both positive and negative vorticity). Tripolar vortices have been also observed (van Heijst, Kloosterziel & Williams 1991; Carton, Flierl & Polvani 1989; Carton & Legras 1994), but are less common. These structures spontaneously emerge and coexist in two-dimensional turbulence (Legras, Santangelo & Benzi 1988).

Explaining this *self-organization* and predicting the resulting flow structure is a challenging problem. The statistical mechanics of the Euler equation (Kuz'min 1982; Miller 1990; Robert 1990; Robert & Sommeria 1991) provides a general framework to tackle this problem. It can be considered as a generalization to continuous vorticity fields of the point-vortex statistical mechanics introduced by Onsager (1949) and developed by Joyce & Montgomery (1973) with the mean field approximation. This theory predicts a statistical equilibrium, which is the most probable outcome of

a complex stirring, with constraints due to the conserved quantities of the system (these are the energy and successive moments of the vorticity probability distribution, and for appropriate geometries, the impulse and angular momentum). A similar statistical theory has been proposed by Lynden-Bell (1967) to justify the observed density profile of collisionless stellar systems (described by the Vlasov equation). This analogy is discussed in detail by Chavanis, Sommeria & Robert (1996).

Various equilibrium structures can be obtained, which generally depend on the shape of the fluid domain. However when the initial field of vorticity $\omega_0(\mathbf{r})$ is purely positive (or purely negative) isolated vorticity structures (monopoles) are predicted (Lundgren & Pointin 1977), with exponential or power-law vorticity decay at large distances. This *self-confinement* is due to the conservation of energy, which restricts vorticity spreading.

In contrast, when $\omega_0(\mathbf{r})$ has both positive and negative values, the formation of isolated structures (in particular dipoles and tripoles) cannot be explained as a global equilibrium: an additional hypothesis of *vorticity confinement* in a subdomain[†] must be assumed (Sommeria 1994). In fact, even in the case of monopoles, the final states resulting from direct numerical simulations (Sommeria, Staquet & Robert 1991) have a more confined vorticity than the predicted global equilibrium. The fit with the statistical theory appears to be excellent only in a core region, containing most of the vorticity. Some vorticity filaments escape this core region, and wrap around it, forming a halo, but vorticity sharply drops to zero beyond this halo.

This confinement can be justified in the framework of the statistical theory by considering kinetic effects. An evolution equation describing the relaxation towards equilibrium is then used (Robert & Rosier 1997). Indeed the relaxation toward equilibrium is due to eddy fluxes associated with local vorticity fluctuations. As these fluctuations vanish at the contact with the unmixed flow, the eddy flux also vanishes and this results in a confinement of the vorticity. In addition, the vortex boundary undergoes strong strain and vorticity filaments are stretched towards finer and finer scales, which further reduces the eddy fluxes. On the basis of these ideas, Robert & Rosier (1997) have obtained a self-organization into dipoles or tripoles, in excellent agreement with direct numerical simulations of slightly viscous flows.

However, the final state is then obtained by solving an evolution equation from a particular initial condition. To reach a more general understanding of the self-organization, we seek here a prediction in terms of a restricted equilibrium state: we idealize the behaviour of the system by assuming that after some mixing with the surrounding fluid, vorticity remains trapped and well stirred inside a bubble, with a given area and a deformable boundary. We are led therefore to our basic assumption: the system eventually organizes into a state of maximum entropy, with the constraints of the conserved quantities, and an additional (kinetic) constraint of a given bubble area. The shape and position of the bubble, as well as the vorticity structure inside the bubble, then result from entropy maximization.

This principle is precisely stated in § 2.1. It leads (in § 2.2) to a well-defined relation-

[†] There is a similar, and even more crucial, problem in the case of stellar systems. Indeed an unbounded isothermal sphere would have an infinite mass. This means that statistical equilibrium cannot exist in the whole space, and is necessarily restricted to some bounded region. The observation of elliptical galaxies or globular clusters confirm this point (see e.g. Hjorth & Madsen 1991). For negative individual energies (corresponding to tightly bound stars) the distribution function is exponential, in agreement with statistical equilibrium. However, close to the escape energy, the distribution function decreases more rapidly (as a power law) and for higher energies the stars escape to infinity and the distribution function sharply drops to zero.

ship between vorticity and stream function which determines the equilibrium state, just like in a bounded domain. The novel aspect is that the boundary condition is not given by an impermeability condition at the wall, but rather by an appropriate matching with the surrounding irrotational flow (§ 2.3). When it is not axisymmetric, the equilibrium vorticity structure moves with a steady velocity, of rotation or translation, and the conserved quantities are expressed (in § 2.4) as integral constraints in the frame of reference moving with the vorticity structure. The determination of the equilibrium state from an arbitrary initial condition is therefore a well-defined problem, provided we introduce a single free parameter, the area achieved by the bubble, which characterizes the kinetic restriction to mixing. We shall see by the study of the second-order variations (§§ 2.5 and 3.5) that this area is, in fact, constrained to a narrow range, beyond which there is no entropy maximum. In this case, we expect the vortex boundary to deform irreversibly, absorbing surrounding fluid, or split into several bubbles, until a suitable area is reached. Therefore, the prediction of the flow organization from an initial state will turn out to be very selective. This selection will yield solutions with continuous (or weakly discontinuous) vorticity at the boundary, a condition not assumed *a priori*.

In a bounded domain, a general algorithm for determining the maximum-entropy state has been developed by Whitaker & Turkington (1994). The generalization to the case of a maximum-entropy bubble would require specific developments. To proceed further with analytical tools, we suppose instead that the relationship between vorticity and stream function is linear. This particular case of statistical equilibrium is not uncommon, as discussed by Chavanis & Sommeria (1996) for a bounded domain. It can be reached for any value of the circulation (first vorticity moment), enstrophy (second vorticity moment), impulse, angular momentum and energy, if the initial condition has the appropriate set of higher-order vorticity moments. With this restriction, we obtain in § 3 an explicit classification of isolated equilibrium structures, involving monopoles, and asymmetric or symmetric dipoles. Remarkably, their selection depends on the conserved quantities only through a single control parameter.

These structures are well-known as particular solutions to the Euler equations (Chaplygin 1902; Lamb 1932; see also Meleshko & van Heijst 1994 for a review). A novelty of our work is to determine which solutions correspond to any given values of the constants of motion. This result, derived in §§ 3.1–3.4, can be used independently of the statistical mechanics formalism developed in § 2. This formalism however provides a justification of their emergence from an initial turbulent state. Furthermore, the condition of maximum entropy imposes a severe selection among these steady solutions, as discussed in § 2.4. The derivation of these stability conditions requires a lengthy analysis of the second-order entropy variations, postponed to § 3.5.

In the linearized limit developed in § 3, the entropy maximization becomes equivalent to a minimum-enstrophy principle. We discuss this link in § 4, comparing our results with the approach of Leith (1984).

2. The maximum-entropy bubble

2.1. Basic assumptions and notation

We consider some initial patch of non-zero vorticity, occupying a domain (\mathcal{D}_0) with area $|\mathcal{D}_0|$, surrounded by irrotational fluid in the infinite plane. The Euler equations are known to develop very complex vorticity filaments, so that this patch is expected

to mix with the surrounding fluid, and to form a mixture filling a new domain (\mathcal{D}). We shall be interested in a coarse-grained description of the vorticity field, with a statistical representation of the unresolved vorticity fluctuations. Accordingly, the domain (\mathcal{D}) must be viewed as a ‘smooth’ enclosure of the patch with non-zero vorticity. The area $|\mathcal{D}| > |\mathcal{D}_0|$ is supposed prescribed because of kinetic restrictions on mixing. However, the shape of this domain is free to vary by large-scale deformation and will be determined by entropy maximization. We assume for simplicity that all the vorticity remains in a single connected bubble. We shall find that statistical equilibrium is not always possible, suggesting in that case an organization into several bubbles. This situation could be analysed by similar methods, but we shall leave it for future work.

The initial vorticity patch is not necessarily uniform, and contains a distribution $\gamma(\sigma)$ of vorticity levels σ , that is $\gamma(\sigma) d\sigma$ is the area occupied by vorticity values between σ and $\sigma + d\sigma$. This area is conserved in time during the mixing process, a consequence of the Euler equation. The global distribution of vorticity levels in the new domain (\mathcal{D}) is then equal to the initial one, except for the level $\sigma = 0$ as an area $|\mathcal{D}| - |\mathcal{D}_0|$ of surrounding irrotational fluid has been incorporated and mixed into the new domain. The resulting distribution in (\mathcal{D}) is then $\gamma_{\mathcal{D}}(\sigma) = \gamma(\sigma) + (|\mathcal{D}| - |\mathcal{D}_0|)\delta(\sigma)$ (where δ is the Dirac distribution). In addition to the total area of each vorticity level, the energy E is also conserved in the process, as well as the angular momentum L and the two components of the impulse \mathbf{P} .

We describe the mixing process using the formalism developed by Robert & Sommeria (1991), with presentation and notation similar to that of Chavanis & Sommeria (1996): a macroscopic (coarse-grained) state is defined by the probability $\rho(\mathbf{r}_o, \sigma)$ of finding the vorticity level σ in a small neighbourhood of the position \mathbf{r}_o . The normalization condition yields, at each point,

$$\int \rho(\mathbf{r}_o, \sigma) d\sigma = 1. \quad (2.1)$$

According to our hypothesis, this probability vanishes outside the domain (\mathcal{D}) for all $\sigma \neq 0$, so that $\rho(\mathbf{r}_o, \sigma) = \delta(\sigma)$ outside (\mathcal{D}). The probability ρ can be physically defined by setting a resolution scale ϵ . In an elementary cell (with area ϵ^2), the probability $\rho(\mathbf{r}_o, \sigma) d\sigma$ is the area proportion with vorticity in the interval $[\sigma, \sigma + d\sigma]$. For an ideal fluid, vorticity contours tend to become more and more finely intertwined as time goes on (this is the most likely outcome of random stirring), so that a good statistical sampling is expected for any given resolution ϵ . The probability ρ is then defined for an infinitesimal resolution ϵ .

In practice we expect that weak viscosity effects eventually smooth out the local vorticity fluctuations, while preserving the locally averaged field of vorticity, expressed in terms of the probability density as

$$\bar{\omega}(\mathbf{r}_o) = \int \rho(\mathbf{r}_o, \sigma) \sigma d\sigma. \quad (2.2)$$

However, we do not need to invoke any viscous effect, and prefer to restrict the theoretical description to an ideal fluid. Then, fine-scale vorticity fluctuations $\tilde{\omega}$, of the same order as the local average $\bar{\omega}$, persist at statistical equilibrium but at infinitesimal scales smaller than a resolution mesh ϵ . The velocity field associated with $\bar{\omega}$ is essentially smooth and is derived from the stream function ψ satisfying

$$\bar{\omega} = -\Delta\psi. \quad (2.3)$$

Local fluctuations of the stream function $\tilde{\psi} \sim \epsilon^2 \tilde{\omega}$ can be neglected. The Poisson equation (2.3) determines ψ if we specify its asymptotic behaviour at large distance. It is dominated by the monopolar term in the expansion of the Biot & Savart law, hence for $r_o \rightarrow +\infty$

$$\psi \sim -\frac{\Gamma}{2\pi} \ln r_o. \quad (2.4)$$

In fact, we are free to introduce an additional constant in this expansion, but we set it to zero. Accordingly, for a given vorticity field $\bar{\omega}$, (2.3) and (2.4) define the stream function unambiguously.

It is then possible to express the conserved quantities as integrals of the macroscopic fields. These are the global probability distribution of vorticity in (\mathcal{D})

$$\gamma_{\mathcal{D}}(\sigma) = \int_{\mathcal{D}} \rho(\mathbf{r}_o, \sigma) d^2 \mathbf{r}_o, \quad (2.5)$$

the energy of the flow

$$E = \frac{1}{2} \int \bar{\omega} \psi d^2 \mathbf{r}_o, \quad (2.6)$$

the angular momentum

$$L = \int \bar{\omega} r_o^2 d^2 \mathbf{r}_o, \quad (2.7)$$

and the two components of the impulse

$$\mathbf{P} = \int \mathbf{r}_o \wedge \mathbf{i}_z \bar{\omega} d^2 \mathbf{r}_o, \quad (2.8)$$

where \mathbf{i}_z is a unit vector normal to the plane of the flow. These three integrals (2.6)–(2.8) can be restricted to the subdomain (\mathcal{D}), as they involve a quantity proportional to the vorticity, which vanishes outside (\mathcal{D}). Note also that in writing (2.6) we have neglected the ‘internal’ energy $\bar{\omega} \tilde{\psi}$, of order $\epsilon^2 \bar{\omega}^2$, much smaller than $\bar{\omega} \psi$, of order $L^2 \bar{\omega}^2$ (see also Robert & Sommeria 1991).

The conservation of the global probability density distribution $\gamma_{\mathcal{D}}$ implies the conservation of all the vorticity moments, including the circulation Γ and the fine-grained enstrophy Γ_2 :

$$\Gamma \equiv \int \gamma_{\mathcal{D}}(\sigma) \sigma d\sigma = \int \bar{\omega}(\mathbf{r}_o) d^2 \mathbf{r}_o, \quad (2.9)$$

$$\Gamma_2 \equiv \int \gamma_{\mathcal{D}}(\sigma) \sigma^2 d\sigma = \int \bar{\omega}^2(\mathbf{r}_o) d^2 \mathbf{r}_o, \quad (2.10)$$

where $\bar{\omega}^2(\mathbf{r}_o) = \int \rho(\mathbf{r}_o, \sigma) \sigma^2 d\sigma$. Notice that Γ_2 has to be distinguished from the coarse-grained enstrophy

$$\Gamma_2^{\text{c.g.}} \equiv \int \bar{\omega}^2(\mathbf{r}_o) d^2 \mathbf{r}_o \quad (2.11)$$

which is not conserved (we have always $\Gamma_2^{\text{c.g.}} \leq \Gamma_2$).

Notice also that the impulse and the angular momentum have been defined from a given arbitrary coordinate origin O . When $\Gamma \neq 0$, a natural origin is the centre of vorticity, from which $\mathbf{P} = 0$. The conservation of the impulse then implies that the centre of vorticity does not move. When $\Gamma = 0$, the impulse \mathbf{P} is independent of the origin and the centre of vorticity is rejected at infinity.

After sufficient time (and random evolution), the system has an overwhelming

probability of achieving a statistical equilibrium obtained by maximizing the mixing entropy

$$S = - \int \rho(\mathbf{r}_o, \sigma) \ln \rho(\mathbf{r}_o, \sigma) d^2 \mathbf{r}_o d\sigma \quad (2.12)$$

with the constraints (2.5)–(2.8) associated with the conservation laws, and with the additional constraint of given area $|\mathcal{D}|$ (due to kinetic restrictions to mixing). The shape of the subdomain (\mathcal{D}) is free in the maximization process, as well as the probability fields $\rho(\mathbf{r}_o, \sigma)$ inside (\mathcal{D}). The entropy expression (2.12) can be obtained as the logarithm of the ‘number’ of possible vorticity configurations associated with the considered macroscopic state. In fact an overwhelming majority of these configurations corresponds to the statistical equilibrium, justifying that it is likely to be reached after complex evolution. This concentration property is at the origin of the predictive power of statistical mechanics in general, and has been proved by Robert (1991) in the case of vorticity fields. The ‘counting’ of the vorticity configurations relies on a regular discretization of space, which can be justified from the dynamics by an invariance theorem, a weak form of the Liouville theorem used in usual statistical mechanics (see the end of §2.3).

To calculate equilibrium states, it will be useful to deal with dimensionless quantities, introducing a unit of length $|\mathcal{D}_0|^{1/2}$ and a unit of time $(|\mathcal{D}_0|/\Gamma_2)^{1/2}$. This is equivalent to making $|\mathcal{D}_0| = \Gamma_2 = 1$ and we will take this convention in the following.

2.2. First-order variations

To take into account the constraints on the entropy maximization, we introduce Lagrange multipliers, so that the first variations satisfy

$$\delta S - \tilde{\beta} \delta E - \int \tilde{\alpha}(\sigma) \delta \gamma_{\mathcal{D}}(\sigma) d\sigma - \int \tilde{\zeta}(\mathbf{r}_o) \delta \left(\int \rho(\mathbf{r}_o, \sigma) d\sigma \right) d^2 \mathbf{r}_o - \tilde{\beta} \frac{\Omega}{2} \delta L + \tilde{\beta} \mathbf{V} \delta \mathbf{P} = 0 \quad (2.13)$$

where $\tilde{\beta}$ is the inverse temperature, $\tilde{\alpha}(\sigma)$ the ‘chemical potential’ of species σ , Ω will be later interpreted as the angular velocity of the subdomain (\mathcal{D}) and \mathbf{V} its translational velocity. The Lagrange multiplier $\tilde{\zeta}(\mathbf{r}_o)$ takes into account the normalization constraint (2.1). It will be useful in the following to work in terms of a ‘free energy’ defined by:

$$J = S - \tilde{\beta} E - \int \tilde{\alpha}(\sigma) \gamma_{\mathcal{D}}(\sigma) d\sigma - \int \tilde{\zeta}(\mathbf{r}_o) \rho(\mathbf{r}_o, \sigma) d\sigma d^2 \mathbf{r}_o - \tilde{\beta} \frac{\Omega}{2} L + \tilde{\beta} \mathbf{V} \mathbf{P}. \quad (2.14)$$

Then, the optimal state can be considered either as a critical point of the entropy for any perturbations conserving the constraints (2.1), (2.5)–(2.8) or equivalently, as a critical point of the free energy ($\delta J = 0$) for any unconstrained perturbations.

As a result of (2.13), the optimal probability density $\rho(\mathbf{r}_o, \sigma)$ in a given domain (\mathcal{D}) is related to the macroscopic stream function ψ by the relationship (see Robert & Sommeria 1991)

$$\rho(\mathbf{r}_o, \sigma) = \frac{1}{Z} g(\sigma) e^{-\tilde{\beta} \sigma \psi'} \quad (2.15)$$

where

$$\psi' \equiv \psi + \frac{1}{2} \Omega r_o^2 - (\mathbf{V} \wedge \mathbf{r}_o)_z + B. \quad (2.16)$$

B is a constant which will be specified later, $g(\sigma) \equiv e^{-\tilde{\alpha}(\sigma) + \tilde{\beta} \sigma B}$ and $Z \equiv e^{\tilde{\zeta}(\mathbf{r}_o) + 1}$. The

normalization condition (2.1) determines the partition function:

$$Z = \int g(\sigma) e^{-\tilde{\beta}\sigma\psi'} d\sigma, \quad (2.17)$$

and the locally averaged vorticity (2.2) is expressed in (\mathcal{D}) by

$$\bar{\omega} = f_{\tilde{\beta},g}(\psi') \quad (2.18)$$

where

$$f_{\tilde{\beta},g}(\psi') \equiv \frac{\int \sigma g(\sigma) e^{-\tilde{\beta}\sigma\psi'} d\sigma}{\int g(\sigma) e^{-\tilde{\beta}\sigma\psi'} d\sigma}. \quad (2.19)$$

This function is always increasing when $\tilde{\beta} < 0$ and decreasing when $\tilde{\beta} > 0$, as shown by Robert & Sommeria (1991). It is therefore invertible, so that ψ' is also a function of $\bar{\omega}$ (except in the degenerate case $\tilde{\beta} = 0$ for which $f_{\tilde{\beta},g}$ is a constant). Notice finally that the function $f_{\tilde{\beta},g}(\psi')$ tends to the extremal values σ_{min} and σ_{max} of the vorticity levels when $\psi' \rightarrow \pm\infty$; in general, however, these bounds are not reached in the flow, as the vorticity σ_{min} or σ_{max} is locally mixed to some extent with the other vorticity levels.

The stream function ψ' describes the flow in a translating or rotating frame of reference (\mathcal{R}') , in which the vorticity is

$$\bar{\omega}' = \bar{\omega} - 2\Omega. \quad (2.20)$$

According to (2.18), the relative vorticity $\bar{\omega}'$ is a function of ψ' , so that the flow is stationary in the moving frame (\mathcal{R}') . This flow is a solution of the equation

$$-\Delta\psi = f_{\tilde{\beta},g}(\psi') \quad (2.21)$$

obtained by stating that the stream function in (2.18) is produced by the vorticity distribution itself, according to (2.3).

2.3. Vorticity confinement and matching with the irrotational background

To determine the equilibrium stream function ψ as a solution of (2.21), we need a boundary condition. In the case of a fixed bounded domain, it is just the impermeability condition $\psi = 0$ at the walls. In the infinite domain, the first idea is to use instead the asymptotic condition (2.4), which is quite possible when the vorticity levels σ are limited to a single sign. In that case global equilibria are obtained as solutions of (2.21), decaying exponentially or with a power law at large distance. Such equilibria are axisymmetric, as studied by Lundgren & Pointin (1977), or Chorin (1994), with point vortex statistics, and are similarly obtained for vortex patches (Sommeria 1994). In this case, vorticity spreading, always favourable for entropy increase, is restricted by the constraint of energy conservation, hence resulting in a self-confined global equilibrium.

However this not possible in general when the vorticity levels have values between $\sigma_{min} < 0$ and $\sigma_{max} > 0$. Indeed the relative stream function behaves at large distance like $\psi' \sim -(\Gamma/2\pi) \ln r_o + \frac{1}{2}\Omega r_o^2 - (\mathbf{V} \wedge \mathbf{r}_o)_z$. This expression tends to $+\infty$ or $-\infty$, except in the particular case $\Gamma = \Omega = \mathbf{V} = 0$. In this case, monopolar and dipolar solutions of (2.21) have been obtained by Pasmanter (1994) (but it is not clear whether they are true entropy maxima). Otherwise, the function $f_{\tilde{\beta},g}$ has an infinite argument at large distance and tends to one of its bounds σ_{min} and σ_{max} . Hence the vorticity does not tend to zero, in contradiction with the hypothesis of a confined structure.

Therefore, global equilibria may exist only for structures involving purely positive (or purely negative) vorticity levels. However, even in these cases, direct numerical simulations indicate that the vorticity is more confined than expected (Sommeria *et al.* 1991). This is why we seek a restricted equilibrium with vorticity confined to a subdomain (\mathcal{D}), with probabilities dropping discontinuously to zero at the boundary of (\mathcal{D}). We may try to justify this structure as a global statistical equilibrium which is not continuous. However, a simple calculation indicates that a local smoothing of the discontinuity, leading to a probability drop over a distance ϵ , will lead to an increase of entropy of order ϵ . In contrast, the integral constraints (like the energy) are changing only to order ϵ^2 , so they are not able to prevent the smoothing (the term $\tilde{\beta}\delta E$ is not able to balance δS in the variation of free energy, except in the particular limit $|\tilde{\beta}| \rightarrow \infty$, obtained for a vorticity patch with an extremal energy, which cannot mix at all, and remains unchanged at equilibrium; see for instance figure 1 of Chavanis & Sommeria (1996)). Therefore we assume that mixing at the edge of (\mathcal{D}) is prevented by an additional constraint (of kinetic origin), acting like a membrane, which preserves the area of (\mathcal{D}), but is freely deformable.

The equilibrium flow inside (\mathcal{D}) is then a solution of (2.21), but we now need a boundary condition. It is clear that in the moving frame of reference (\mathcal{R}'), the boundary ($\partial\mathcal{D}$) must be a streamline, otherwise the vorticity would be advected outside the domain and the flow would not be stationary anymore. This implies that ψ' is necessarily constant on ($\partial\mathcal{D}$). We have obtained this criterion by a dynamical argument, but it also results directly from the condition that the entropy must be maximum with respect to small deformations of the domain shape. We now justify this result with simple arguments (and will derive it more rigorously in §2.5, considering also the second variations of the entropy).

As a particular deformation, we take a fluid particle somewhere at the boundary of the subdomain (on the inner side), and put it elsewhere on the boundary (on the outer side). During this displacement, we conserve the value $\bar{\omega}$ of the fluid particle, as well as its local probability distribution. Therefore the constraints on $\gamma_{\mathcal{D}}(\sigma)$ and the normalization condition are satisfied, and the entropy is unchanged. The condition of equilibrium then implies that the free energy

$$J_d \equiv -\tilde{\beta} \left(E + \frac{1}{2}\Omega L - \mathbf{V} \cdot \mathbf{P} \right) = -\frac{1}{2}\tilde{\beta} \int \bar{\omega}\psi d^2\mathbf{r}_o - \tilde{\beta}\frac{1}{2}\Omega \int \bar{\omega}r_o^2 d^2\mathbf{r}_o + \tilde{\beta} \int \bar{\omega}(\mathbf{V} \wedge \mathbf{r}_o)_z d^2\mathbf{r}_o \quad (2.22)$$

is conserved to first order for any displacement ($\delta J_d = 0$). We may consider that the particle has the elementary energy $\bar{\omega}\psi$ in the stream function ψ due to all the other fluid particles (like a potential energy for a charge in an electrostatic field), an elementary angular momentum $\bar{\omega}r_o^2$ and an elementary impulse $\bar{\omega}\mathbf{r}_o \wedge \mathbf{i}_z$. The resulting contribution to the free energy (2.22) is proportional to $\bar{\omega}\psi + \frac{1}{2}\Omega\bar{\omega}r_o^2 - \mathbf{V} \cdot \bar{\omega}\mathbf{r}_o \wedge \mathbf{i}_z = \bar{\omega}\psi'$. Therefore if $\bar{\omega} \neq 0$ somewhere on the boundary, the condition $\delta J_d = 0$ implies that $\psi' = \text{const.}$ on the boundary ($\partial\mathcal{D}$) (this is analogous to the condition of a constant potential on the free surface of a liquid at equilibrium in a gravitational field). This condition still holds if $\bar{\omega} = 0$ along the whole boundary since ψ' is a function of $\bar{\omega}$ at equilibrium. Therefore in all cases ψ' must be constant on the boundary of the subdomain (\mathcal{D}), and we can always take $\psi' = 0$ by an appropriate choice of B in the definition (2.16).

In summary, for a given subdomain (\mathcal{D}) and for given Lagrange multipliers, the

flow inside (\mathcal{D}) is determined as a solution of

$$-\Delta\psi' + 2\Omega = f_{\tilde{\beta},g}(\psi') \quad \text{with} \quad \psi' = 0 \quad \text{on} \quad (\partial\mathcal{D}). \quad (2.23)$$

This equation has in general several solutions, and the selection among them is obtained by considering the second-order variations of the entropy, as discussed in §2.5.

Outside (\mathcal{D}), the flow remains irrotational, and is uniquely determined as a solution of the Laplace equation

$$-\Delta\psi = 0 \quad \text{with} \quad \psi = -\frac{1}{2}\Omega r_o^2 + (\mathbf{V} \wedge \mathbf{r}_o)_z - B \quad \text{on} \quad (\partial\mathcal{D}) \quad (2.24)$$

and with the additional condition (2.4) at large distance. The boundary condition corresponds to $\psi' = 0$ and expresses the continuity of ψ at the boundary of (\mathcal{D}) (or, equivalently, the continuity of the normal velocity component). Notice that the constant B is not arbitrary and will be set by the matching between the inside and the outside.

In addition, the continuity of the tangential velocity component must be satisfied. To express this condition, we introduce curvilinear coordinates (χ, ζ) where χ is the curvilinear abscissa along the boundary (in the trigonometric direction), and ζ the outward normal coordinate. We define \mathbf{i}_ζ and \mathbf{i}_χ as the corresponding normal and tangential unit vectors. With these notations, the continuity of the tangential velocity implies

$$\left(\frac{\partial\psi'}{\partial\zeta}\right)_{\text{inside}} = \left(\frac{\partial\psi}{\partial\zeta}\right)_{\text{outside}} + (\Omega \wedge \mathbf{r}_o + \mathbf{V})\mathbf{i}_\chi \quad \text{on} \quad (\partial\mathcal{D}). \quad (2.25)$$

This additional condition determines in principle the shape of the boundary. However, this shape may be very difficult to obtain explicitly and numerical methods must be used in general.

The Lagrange multipliers are given only indirectly, through the integral constraints stemming from the conservation laws (2.5)–(2.8). These are expressed in terms of the absolute coordinates \mathbf{r}_o , and it is necessary to express them in the relative coordinates, linked with the domain (\mathcal{D}). This will be discussed in §2.4.

The stream function solution of (2.24) corresponds to the inviscid flow produced around a solid body undergoing a rotation at angular velocity Ω and a translation at velocity \mathbf{V} , while (2.23) describes a steady flow in the frame of reference moving with this body. A set of equivalent equilibrium states will be predicted describing the same structure translated to or rotated at different positions. The Euler equation then indicates that, as time goes on, this structure will steadily travel among this set of equilibrium states. Notice that the statistical theory does not explicitly describe time evolution, and involves the Euler equation only through its conservation laws. The fact that the equilibrium states correspond to steady solutions of the Euler equation appears therefore as a remarkable feature of the theory. This property guarantees that the system will remain in the set of equilibrium states once it is reached. This dynamical justification of the theory, corresponding to the invariance theorem proved by Robert (1991), can be considered as a weak form of the Liouville theorem underlying the usual statistical mechanics (but not available for a fluid). It is interesting to notice that this justification persists in the extension of the theory that we use here, considering deformations of the domain (\mathcal{D}) with the additional constraint of a fixed area.

2.4. Expressions for the integral constraints in the relative frame of reference

We have seen that the equilibrium structures are not stationary in the initial frame of reference but move with a combined motion of rotation and translation, corresponding to the relation (2.16) between ψ and ψ' . In fact, the motion is either a pure rotation or a pure translation. Indeed, when $\Omega \neq 0$, the term in V can always be suppressed by an appropriate choice of the origin, yielding a pure rotation, and when $\Omega = 0$ the motion is, of course, a pure translation.

In terms of the given conserved quantities, the case of a translation corresponds to $\Gamma = 0$ and $\mathbf{P} \neq 0$, as for instance in a symmetric dipole. Indeed a rotation would be incompatible with the conservation of the impulse \mathbf{P} in this case (the vector would rotate). The case of a rotation corresponds to the alternative possibility, $\Gamma \neq 0$ or $\Gamma = 0$ with $\mathbf{P} = 0$ (for instance in an asymmetric dipole or monopole). This rotation occurs around the centre of vorticity when $\Gamma \neq 0$, and the impulse is zero with this coordinate origin, so its conservation does not forbid rotation.

This classification can be also obtained directly, without reference to dynamical arguments. Indeed, the following relation is established in Appendix A:

$$\Omega \mathbf{P} = \Gamma \mathbf{V}. \quad (2.26)$$

From this relation, it follows immediately that if $\Gamma = 0$ and $\mathbf{P} \neq 0$, then $\Omega = 0$, so the motion is a translation. By contrast, if $\Gamma \neq 0$, and the origin is chosen at the centre of vorticity, so that $\mathbf{P} = 0$, then $\mathbf{V} = 0$, and the motion is a rotation.

The case $\Gamma = 0$ and $\mathbf{P} = 0$ can be treated using another relation, shown in Appendix A for a translating structure:

$$\mathbf{P} = C_{\mathcal{D}} |\mathcal{D}| \mathbf{V} \quad (2.27)$$

where $C_{\mathcal{D}}$ is a constant depending only on the domain shape ($C_{\mathcal{D}} = 2$ for the disk). This is analogous to the classical relation between momentum and velocity for a particle of mass $C_{\mathcal{D}} |\mathcal{D}|$. As a consequence of (2.27), the structure cannot translate if $\mathbf{P} = 0$, and is necessarily rotating around some centre (even if $\Gamma = 0$), or remains at rest.

In the following, we shall restrict the discussion to the cases $\Gamma \neq 0$ (and recover the case $\Gamma = 0$ as a particular limit). According to the previous discussion, it is convenient to take the origin O at the centre of vorticity, around which the structure will rotate, so that $\mathbf{P} = 0$ and $\mathbf{V} = 0$. On the other hand, it is also useful to introduce the *proper* impulse \mathbf{P}' and angular momentum L' , defined in the moving frame of reference by

$$L' = \int_{\mathcal{D}} \bar{\omega}' r^2 d^2 \mathbf{r}, \quad (2.28)$$

$$\mathbf{P}' = \int_{\mathcal{D}} \mathbf{r} \wedge \mathbf{i}_z \bar{\omega}' d^2 \mathbf{r}. \quad (2.29)$$

The position \mathbf{r} is then determined from an origin C linked with (\mathcal{D}) , see figure 1, defined as the centre of mass of the domain, i.e. $\langle \mathbf{r} \rangle = 0$, where $\langle \cdot \rangle = (1/|\mathcal{D}|) \int_{\mathcal{D}} \cdot d^2 \mathbf{r}$ represents the domain average. When the proper impulse \mathbf{P}' is zero (this is the case in particular for monopoles and tripoles), the centre of the vortex C coincides with the centre of vorticity O and the structure is motionless (it can however rotate around its own axis). In contrast, when $\mathbf{P}' \neq 0$ (this is the case for the dipoles), the structure rotates around the centre of vorticity with a radius of rotation R (we obtain a translating structure when $R \rightarrow \infty$).

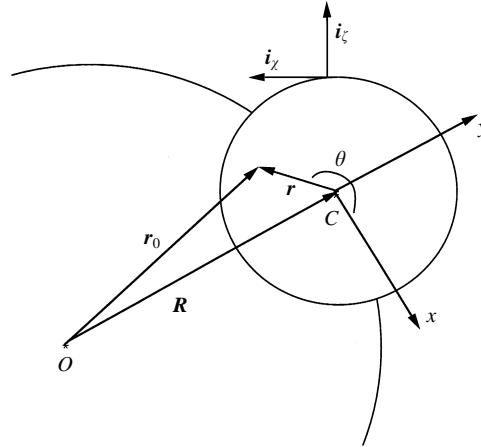


FIGURE 1. Sketch of the coordinates attached to the fixed origin O , and the coordinates attached to the origin C , moving with the vortex.

These quantities L' and \mathbf{P}' intrinsically characterize the vorticity structure, but are not directly determined by the initial conditions, in contrast to \mathbf{P} and L . To relate these two sets of quantities, we introduce the (vector) distance $\mathbf{R} = \mathbf{OC}$, so that $\mathbf{r}_o = \mathbf{r} + \mathbf{R}$. Using (2.29) and (2.8) with $\mathbf{P} = 0$ (since O is the centre of vorticity) and $\langle \mathbf{r} \rangle = 0$ (since C is the centre of mass), we find

$$\mathbf{P}' = -\Gamma \mathbf{r} \wedge \mathbf{i}_z \quad (2.30)$$

and verify that the impulse \mathbf{P}' lies along the motion of the vortex (it is tangent to its circular trajectory). We now introduce a Cartesian system of coordinates (x, y) with origin at the centre C , y along \mathbf{OC} and x perpendicular (see figure 1). In that case, \mathbf{P}' has only a component along x :

$$P' = \int \bar{\omega}' y d^2 \mathbf{r} = -\Gamma R. \quad (2.31)$$

Finally, the relation between the angular momentum of the vortex L' and the global angular momentum L is obtained by expanding (2.7), yielding

$$L = \Gamma R^2 + L' + 2\Omega \langle r^2 \rangle |\mathcal{D}| + 2RP' \quad (2.32)$$

or, using (2.31),

$$L = L' + 2\Omega \langle r^2 \rangle |\mathcal{D}| - P'^2 / \Gamma. \quad (2.33)$$

We also define the proper energy $E' \equiv \frac{1}{2} \int_{\mathcal{D}} \psi' \bar{\omega}' d^2 \mathbf{r}$, related to E using (2.16) (with $\mathbf{V} = 0$), which leads to

$$E = E' + \Omega \langle \psi' \rangle |\mathcal{D}| - \frac{\Omega L}{4} - \frac{\Gamma B}{2}. \quad (2.34)$$

These two relations (2.33), (2.34) provide constraints on the solution of (2.23) in the interior, which replace the constraints on energy and angular momentum used in a fixed domain. An additional set of constraints is provided by the conservation of the global vorticity distribution (2.5), in the same way as in a fixed domain (these constraints will be greatly simplified in the case of strong mixing considered in §3). The interior solution is therefore self-consistently defined as a solution of (2.23), provided we prescribe the constant B and the shape of the domain. Once a solution

ψ' and the corresponding Lagrange multipliers $\tilde{\beta}$ and Ω have been determined, the radius of rotation R is given by (2.31). Then, the exterior solution is obtained as a solution of (2.24), with $V = 0$. The matching condition (2.25) then constrains the domain shape and determines the constant B . Several solutions can be obtained by this procedure, as in the case of a fixed domain. The consideration of the second variations of the entropy will allow us to make a selection among them.

The previous relations have been obtained under the assumption $\Gamma \neq 0$. When $\Gamma = 0$, the impulse \mathbf{P} is independent of the origin and the centre of vorticity is rejected to infinity. In the limit $\Gamma \rightarrow 0$ and $\mathbf{P} \neq 0$, the relations (2.26) and (2.31) yield

$$V = -\Omega R \quad (2.35)$$

with $R \rightarrow \infty$ and $\Omega \rightarrow 0$. As a result, a translating structure can be viewed as a rotating structure with an infinite radius of rotation. In that case, the angular momentum is dominated by the product ΓR^2 and (2.33) reduces to

$$\Gamma L = -P^2 \quad (2.36)$$

with $\Gamma \rightarrow 0$ and $L \rightarrow \infty$.

2.5. Second-order variations

The previous solutions cancel the first constrained variations of the entropy (they are critical points), but are not necessarily maxima. To settle this, we have to check whether the second variations $\delta^2 S$ are negative for any perturbation that strictly conserves the constraints. This is equivalent to checking that the second variations of the free energy (defined with the Lagrange multipliers of the equilibrium state) are strictly negative ($\delta^2 J < 0$) for any small perturbation $\delta\rho(\mathbf{r}_o, \sigma)$ which does not change the constraints to first order. Notice that our 'free energy' (2.14) is defined for convenience with the opposite sign from usual thermodynamics, so that it must be maximum at equilibrium, like the constrained entropy.

Let us first consider perturbations $\delta\rho(\mathbf{r}_o, \sigma)$ of the equilibrium probability distributions $\rho(\mathbf{r}_o, \sigma)$ within a fixed domain (\mathcal{D}). A Taylor expansion of the general expressions for the energy (2.6) and entropy (2.12) yields

$$\delta^2 J = -\frac{1}{2} \int \frac{(\delta\rho)^2}{\rho} d^2\mathbf{r}_o d\sigma - \frac{1}{2} \tilde{\beta} \int \delta\psi \delta\bar{\omega} d^2\mathbf{r}_o. \quad (2.37)$$

The other constraints are linear in ρ so their second variations vanish. Here, ρ and $\tilde{\beta}$ refer to the local extremum that we want to perturb. The integral of the second term can be written, by an integration by parts, as $\int (\nabla\delta\psi)^2 d^2\mathbf{r}$, which is always positive. Therefore, when $\tilde{\beta}$ is positive, $\delta^2 J$ is negative and the (single) critical point is a maximum. It remains a maximum as long as $\tilde{\beta}$ is greater than the first eigenvalue of the Laplacian $\tilde{\beta}_{01}$, as stated by Robert & Sommeria (1991). For smaller values of $\tilde{\beta}$, the selection of entropy maxima is not given by any simple criterion (at least in the general case). In §3, we will consider a particularly interesting limit of the theory in which (2.37) can be simplified and yields an illuminating condition of stability.

Furthermore, we now demand that the optimal distribution (2.15) remains an entropy maximum when we deform slightly the boundary ($\partial\mathcal{D}$) while keeping the area $|\mathcal{D}|$ unchanged. This deformation is a continuous area-preserving displacement of fluid particles, without changing their respective probability distribution. Therefore the constraints on $\gamma_{\mathcal{D}}(\sigma)$ and local normalization are satisfied by the deformation, and the entropy is unchanged. The corresponding condition of equilibrium is thus that the first variation of the free energy J_d , defined by (2.22), vanishes for any deformation

and that $\delta^2 J_d < 0$ for the deformations that do not change the constraints to first order. In contrast, any deformation leading to $\delta^2 J_d > 0$ will allow the entropy to increase (by internal mixing) while globally conserving the constraints.

To describe the area-preserving fluid displacement, we introduce a ‘velocity’ field $\mathbf{U}(\mathbf{r}_o, \tau)$ depending on a small ‘time’ parameter τ . We impose $\nabla \cdot \mathbf{U} = 0$ in order to preserve areas during the displacement. The probability densities (and thus the locally averaged vorticity) are purely advected by this imposed flow and therefore satisfy the transport equation

$$\frac{\partial \bar{\omega}}{\partial \tau} + \nabla \cdot (\bar{\omega} \mathbf{U}) = 0. \quad (2.38)$$

The corresponding energy variation is

$$\frac{dE}{d\tau} = \frac{1}{2} \left(\int \frac{\partial \bar{\omega}}{\partial \tau} \psi d^2 \mathbf{r}_o + \int \bar{\omega} \frac{\partial \psi}{\partial \tau} d^2 \mathbf{r}_o \right) \quad (2.39)$$

where integration is over the whole space. The second term on the right-hand side is equal to the first one, as can be shown by an integration by parts, assuming $\partial \psi / \partial \tau \rightarrow 0$ at large distance. This is justified by the fact that the circulation Γ is unchanged by the deformation, and so is the asymptotic condition (2.4). Therefore, the variation of the free energy (2.22) is just

$$\frac{dJ_d}{d\tau} = -\tilde{\beta} \int \frac{\partial \bar{\omega}}{\partial \tau} \psi' d^2 \mathbf{r}_o \quad (2.40)$$

where integration is again over the whole space[†]. An integration by parts and the use of (2.38) allows us to rewrite this variation as

$$\frac{dJ_d}{d\tau} = -\tilde{\beta} \int_{\mathcal{D}(\tau)} \bar{\omega} \mathbf{U} \cdot \nabla \psi' d^2 \mathbf{r}_o. \quad (2.41)$$

Now, the integrand remains finite at the boundary (unlike in (2.40) when $\bar{\omega}$ is not continuous), so we can restrict the integration to the domain $\mathcal{D}(\tau)$ resulting from the deformation of (\mathcal{D}) at ‘time’ τ . By analogy with electrostatics, a physical interpretation of (2.41) is that during a ‘time’ $d\tau$, each fluid particle with ‘charge’ $\bar{\omega}$ undergoes the small displacement $\mathbf{U} d\tau$ and feels a change of ‘potential’ $\delta \psi' = \mathbf{U} \cdot \nabla \psi' d\tau$, changing its free energy by the amount $-\tilde{\beta} \bar{\omega} \delta \psi'$.

To first order in τ the variation of J_d is just $\delta J_d = \tau I(0)$, where $I(\tau) \equiv dJ_d/d\tau$. The integral in (2.41) at $\tau = 0$ corresponds to the equilibrium state, for which ψ' is a function $h \equiv f_{\tilde{\beta}, g}^{-1}$ of $\bar{\omega}$, see (2.19). Therefore $\bar{\omega} \nabla \psi'$ can be written as $\nabla H(\bar{\omega})$, where H is a primitive of the function $\bar{\omega} h'(\bar{\omega})$. Using an integration by parts and the incompressibility of \mathbf{U} , the first variation can be expressed as a contour integral around the equilibrium boundary:

$$\delta J_d = -\tilde{\beta} \tau \oint_{\partial \mathcal{D}} H(\bar{\omega}) U_\zeta d\chi. \quad (2.42)$$

The condition that J_d is an extremum when we deform the boundary implies that $\delta J_d = 0$ for any incompressible field \mathbf{U} . This is only possible if $\bar{\omega}$, or equivalently ψ' , is constant along the boundary (indeed, the integral in (2.42) is then proportional to

[†] Since $\bar{\omega}$ may be discontinuous at the boundary of the domain, $\partial \bar{\omega} / \partial \tau$ then becomes infinite as the boundary of the domain moves. However, (2.40) is still well defined if we slightly smooth the vorticity at the boundary (or use the theory of distributions).

the flux of \mathbf{U} which vanishes, due to the incompressibility condition). Therefore, we recover the condition that $(\partial\mathcal{D})$ must be a streamline in the moving frame (see §2.3).

The second-order variation is $\delta^2 J_d = (\tau^2/2)I'(0)$. The ‘time’ derivative of the function $I(\tau)$ can be calculated by expanding the integral (2.41) over the infinite plane, and is simply

$$I'(\tau) = -\tilde{\beta} \int \frac{\partial}{\partial \tau} (\overline{\omega} \mathbf{U} \cdot \nabla \psi') d^2 \mathbf{r}_o. \quad (2.43)$$

Making use of (2.38) we obtain the equivalent form

$$I'(\tau) = -\tilde{\beta} \left\{ \int_{\mathcal{D}(\tau)} \overline{\omega} \mathbf{U} \cdot \nabla \left(\frac{\partial \psi}{\partial \tau} + \mathbf{U} \cdot \nabla \psi' \right) d^2 \mathbf{r}_o + \int_{\mathcal{D}(\tau)} \overline{\omega} \frac{\partial \mathbf{U}}{\partial \tau} \cdot \nabla \psi' d^2 \mathbf{r}_o \right\} \quad (2.44)$$

and we can now restrict the integration to the subdomain $\mathcal{D}(\tau)$ for the same reason as before. We need to evaluate this quantity for $\tau = 0$. After an integration by parts, the second integral can be rewritten $\oint_{\partial\mathcal{D}} H(\overline{\omega})(\partial U_\zeta / \partial \tau) d\chi$, which vanishes since $\overline{\omega}$ is constant on the equilibrium boundary and \mathbf{U} is incompressible at all ‘times’ (so the flux $\oint_{\partial\mathcal{D}} (\partial U_\zeta / \partial \tau) d\chi$ is zero). Consequently, the second-order variation of the free energy can be written in terms of just the field \mathbf{U} (at $\tau = 0$) as

$$\delta^2 J_d = -\tilde{\beta} \frac{\tau^2}{2} \int_{\mathcal{D}} \overline{\omega} \mathbf{U} \cdot \nabla (\Psi + h'(\overline{\omega}) \nabla \cdot (\overline{\omega} \mathbf{U})) d^2 \mathbf{r}_o \quad (2.45)$$

where $\Psi \equiv \partial \psi / \partial \tau$ is defined from \mathbf{U} as the (unique) solution of the linear problem:

$$\left. \begin{aligned} \Delta \Psi &= \nabla \cdot (\overline{\omega} \mathbf{U}) \quad \text{inside } (\mathcal{D}), \\ \Delta \Psi &= 0 \quad \text{outside } (\mathcal{D}), \\ \Psi &\rightarrow 0 \quad \text{for } \mathbf{r}_o \rightarrow \infty, \\ \Psi_{\text{inside}} &= \Psi_{\text{outside}} \quad \text{on } \partial\mathcal{D}, \\ \left(\frac{\partial \Psi}{\partial \zeta} \right)_{\text{outside}} - \left(\frac{\partial \Psi}{\partial \zeta} \right)_{\text{inside}} &= -\overline{\omega} U_\zeta \quad \text{on } \partial\mathcal{D}. \end{aligned} \right\} \quad (2.46)$$

The field Ψ can be viewed as the stream function induced by the superposition of a vorticity sheet $\overline{\omega} U_\zeta$ (due to the deformation of the boundary) and a field created by the bulk source $\nabla \cdot (\overline{\omega} \mathbf{U})$ (due to internal rearrangement). The condition of maximum entropy is satisfied when $\delta^2 J_d \leq 0$ for any divergenceless field \mathbf{U} which keeps the constraints unchanged to first order. Since $\delta E = -\frac{1}{2} \Omega \delta L + \mathbf{V} \delta \mathbf{P}$ to first order (corresponding to $\delta J_d = 0$), it is only necessary to demand that $\delta L = \delta \mathbf{P} = 0$. Using (2.7), (2.8), (2.38) and an integration by parts, we can write these first-order variations as

$$\delta L = \int_{\mathcal{D}} \overline{\omega} \mathbf{U} \cdot \mathbf{r}_o d^2 \mathbf{r}_o = 0, \quad (2.47)$$

$$\delta \mathbf{P} = \int_{\mathcal{D}} \mathbf{U} \wedge \mathbf{i}_z \overline{\omega} d^2 \mathbf{r}_o = 0. \quad (2.48)$$

In practice, it is very difficult to show that a structure is stable, because we would have to consider the effect of any deformation field \mathbf{U} satisfying $\nabla \cdot \mathbf{U} = 0$ and (2.47), (2.48). In contrast, a single perturbation which increases the free energy is sufficient to assert that a structure is *not* stable. Hence, our strategy is to find some relevant deformation \mathbf{U} which will destabilize a large number of solutions (2.15). Rather than choosing a deformation field \mathbf{U} , it may be more convenient to choose the value of the source:

$$\lambda(\mathbf{r}_o) \equiv \nabla \cdot (\overline{\omega} \mathbf{U}). \quad (2.49)$$

Indeed, we can express the previous problem in terms of λ only. First of all, we notice that the value of U_ζ on the boundary is simply proportional to λ :

$$U_\zeta = \frac{\lambda}{\partial\bar{\omega}/\partial\zeta} \quad \text{on } (\partial\mathcal{D}) \quad (2.50)$$

since $\bar{\omega} = f(\psi')$ is constant on the boundary (so that $\partial\bar{\omega}/\partial\chi = 0$) and $\nabla \cdot \mathbf{U} = 0$. As a result, the field Ψ solution of the problem (2.46) depends only on λ . The second variations (2.45) of the free energy can be rewritten with an integration by parts as

$$\delta^2 J_d = -\tilde{\beta} \frac{\tau^2}{2} \left\{ \oint_{\partial\mathcal{D}} (\Psi + h'(\bar{\omega})\lambda)\bar{\omega}U_\zeta d\chi - \int_{\mathcal{D}} (\Psi + h'(\bar{\omega})\lambda)\lambda d^2\mathbf{r}_o \right\} \quad (2.51)$$

which, once again, depend only on λ . This is true also for the first-order constraints (2.47), (2.48) which can be rewritten

$$\delta L = \oint \bar{\omega} r_o^2 U_\zeta d\chi - \int \lambda r_o^2 d^2\mathbf{r}_o = 0, \quad (2.52)$$

$$\delta \mathbf{P} = \oint \mathbf{r}_o \wedge \mathbf{i}_z \bar{\omega} U_\zeta d\chi - \int \lambda \mathbf{r}_o \wedge \mathbf{i}_z d^2\mathbf{r}_o = 0. \quad (2.53)$$

Therefore, we can express the whole problem in terms of λ without solving explicitly equation (2.49). Nevertheless, if we want to take λ as a perturbation, we must prove the existence of a corresponding incompressible field \mathbf{U} . We now derive the conditions that λ must fulfil to be associated with an incompressible velocity field. Since $\nabla \cdot \mathbf{U} = 0$, we can introduce a stream function ϕ such that $\mathbf{U} = -\mathbf{i}_z \wedge \nabla\phi$. Let us also introduce a set of orthogonal curvilinear coordinates (ξ_1, ξ_2) where ξ_1 is normal to the streamlines of the vortex (in the rotating frame) and ξ_2 is along them. Let us denote the corresponding unit vectors by \mathbf{e}_1 and \mathbf{e}_2 . In term of these coordinates, a small displacement can be written

$$d\mathbf{x} = h_1 d\xi_1 \mathbf{e}_1 + h_2 d\xi_2 \mathbf{e}_2 \quad (2.54)$$

and equation (2.49) takes the equivalent form

$$\lambda = \frac{1}{h_1 h_2} \left(\frac{\partial\bar{\omega}}{\partial\xi_1} \frac{\partial\phi}{\partial\xi_2} - \frac{\partial\bar{\omega}}{\partial\xi_2} \frac{\partial\phi}{\partial\xi_1} \right). \quad (2.55)$$

Now, we have a relationship $\bar{\omega} = f_{\tilde{\beta},g}(\psi')$ between vorticity and relative stream function at equilibrium. Moreover, by construction of our curvilinear system of coordinates ψ' depends only on ξ_1 . Accordingly, (2.55) reduces to

$$\lambda = \frac{1}{h_2} f'_{\tilde{\beta},g}(\psi') \frac{\partial\phi}{\partial\xi_2} \left(\frac{1}{h_1} \frac{\partial\psi'}{\partial\xi_1} \right) \quad (2.56)$$

and the last term is nothing but the relative velocity of the flow $\mathbf{u}' = -\mathbf{i}_z \wedge \nabla\psi'$. Thus, (2.49) is equivalent to

$$\frac{\partial\phi}{\partial\xi_2} = -\frac{h_2 \lambda}{f'_{\tilde{\beta},g}(\psi') \mathbf{u}'}. \quad (2.57)$$

We know from §2.2 that $f_{\tilde{\beta},g}$ is strictly monotonic; hence, $f'_{\tilde{\beta},g}$ never vanishes (if $\tilde{\beta} \neq 0$), so this equation has a solution for ϕ (and consequently for \mathbf{U}) if:

- (i) $\lambda = 0$ at the points where the velocity vanishes (so that λ/u' remains finite);

(ii) the integral of (2.57) is zero along a streamline, namely

$$\oint \frac{\lambda}{u'} dl = 0. \quad (2.58)$$

When these two conditions are fulfilled, we can use λ as a perturbation (instead of U) and investigate its effect on the vortex stability. This study can be performed analytically in the linearized limit (see §3) and will yield an illuminating condition of stability.

3. The linearized limit

3.1. The linearized equilibrium solutions

We now consider the particular case of a linear relationship $f_{\tilde{\beta},g}$ between vorticity and relative stream function inside the subdomain (\mathcal{D}), so that (2.23) takes the form of a Helmholtz equation:

$$\Delta\psi' + k^2\psi' = k^2\langle\psi'\rangle - \frac{\Gamma'}{|\mathcal{D}|} \quad \text{with} \quad \psi' = 0 \quad \text{on} \quad (\partial\mathcal{D}). \quad (3.1)$$

The right-hand-side constant has been written in terms of the domain average $\langle\psi'\rangle$ and the circulation $\Gamma' = \Gamma - 2\Omega|\mathcal{D}|$ in the relative frame of reference, so as to directly satisfy the constraint on the circulation.

This linearized condition is rigorously obtained from the statistical theory for appropriate values of the conserved quantities, which are commonly approached. Indeed, such a linear relationship (together with a Gaussian local probability distribution of vorticity) is obtained by maximizing entropy with any given value of circulation, enstrophy, energy, impulse and angular momentum (removing the constraints on the higher-order vorticity moments). This is therefore the result of the complete statistical theory for an initial condition with the optimal choice of higher-order vorticity moments. A linear relationship is also approached for any vorticity distribution, in the appropriate range of energy. In this limit of strong mixing, discussed by Chavanis & Sommeria (1996), a systematic expansion in $\tilde{\beta}\sigma\psi'$ yields (3.1) with the relation

$$-k^2|\mathcal{D}| = \left(1 - \frac{\Gamma^2}{|\mathcal{D}|}\right) \tilde{\beta} \equiv \beta \quad (3.2)$$

(in writing (3.1), we have assumed $\tilde{\beta} < 0$ and we will see how to extend the results to the case of positive temperatures).

The temperature $\tilde{\beta}$ (or wavenumber k) and the angular velocity Ω (or relative circulation Γ') must be related to the integral constraints E , Γ , L by solving the system (2.33), (2.34). In the linearized approximation, this system takes the form

$$L = |\mathcal{D}|k^2(\langle\psi'r^2\rangle - \langle\psi'\rangle\langle r^2\rangle) + \Gamma\langle r^2\rangle - P'^2/\Gamma, \quad (3.3)$$

$$E = \frac{1}{2}|\mathcal{D}|k^2(\langle\psi'^2\rangle - \langle\psi'\rangle^2) + \frac{1}{2}\Gamma\langle\psi'\rangle - \frac{1}{4}\Omega L - \frac{1}{2}B\Gamma. \quad (3.4)$$

The problem (3.1) can be classically solved in term of Bessel functions for a circular domain (\mathcal{D}) with given radius a , while the irrotational outside flow is determined by (2.24). It happens that the matching condition (2.25) can be satisfied both for monopole and dipole solutions (Chaplygin 1902; Lamb 1932), for given parameters Ω and k . We shall determine here the set of solutions corresponding to the given conserved quantities L , E and Γ . This is a non-trivial problem in itself (even without reference to the formalism of the statistical theory).

In a circular domain, the general solution of the Helmholtz equation (3.1) is given by

$$\psi' = \langle \psi' \rangle - \frac{\Gamma'}{\pi\alpha^2} + \sum_n a_n J_n(kr) \sin(n\theta + \delta_n) \tag{3.5}$$

where $\alpha \equiv ka$ is a shorthand notation and J_n is the Bessel function of order n (we have excluded Neumann functions because they would lead to divergencies in the core of the vortex).

Outside (\mathcal{D}), the flow is irrotational and we must solve the Laplace equation (2.24) with suitable boundary conditions, namely

$$\left. \begin{aligned} -\Delta\psi &= 0, \\ \psi(a, \theta) &= -\Omega Ra \sin \theta - \frac{1}{2}\Omega(a^2 + R^2) - B, \\ \psi &\sim -\frac{\Gamma}{2\pi} \ln r \quad (r \rightarrow \infty). \end{aligned} \right\} \tag{3.6}$$

This problem is straightforward; the stream function outside the vortex is

$$\psi = -\frac{\Gamma}{2\pi} \ln r - \frac{\Omega Ra^2}{r} \sin \theta \tag{3.7}$$

and the compatibility of (3.7) with the boundary condition of (3.6) imposes

$$B = \frac{\Gamma}{2\pi} \ln a - \frac{1}{2}\Omega(a^2 + R^2). \tag{3.8}$$

Using (3.7) and recalling that $V = 0$ (since we take the origin at the centre of vorticity), the matching condition (2.25) reduces to

$$\frac{\partial\psi'}{\partial r}(a^-, \theta) = 2\Omega R \sin \theta - \frac{\Gamma'}{2\pi a}. \tag{3.9}$$

This must be completed by the boundary condition $\psi'(a) = 0$. Clearly, these conditions cannot be satisfied conjointly by the modes $n > 1$ in the expansion (3.5). Therefore, a circular boundary is only suitable for monopoles ($n = 0$) or dipoles ($n = 1$) (to our knowledge, it is the only possible shape for these structures in the linearized limit). Tripoles and higher-order modes have a more complicated shape and will not be considered in this article. However, in §3.4, we suggest that they are not stable anyway in the linearized limit.

The case of monopoles and dipoles is discussed in detail in §3.2 and 3.3. According to (3.1), (3.3) and (3.4) the only conserved quantities that we have to take into account in the limit of strong mixing are the energy E , the circulation Γ and the angular momentum L (the higher-order moments Γ_n of the vorticity are irrelevant). Moreover, it will turn out that the structure of the equilibrium state depends in fact on a *single* control parameter:

$$\Upsilon = \frac{4\pi E}{\Gamma^2} + \frac{1}{2} \ln \left| \frac{L}{\Gamma} \right|. \tag{3.10}$$

This is a great advantage of the limit of strong mixing which isolates the relevant constraints and permits a neat classification of the equilibrium states.

3.2. Monopoles

The axisymmetric solutions of the Helmholtz equation (3.1) are

$$\psi' = \frac{\Gamma'}{2\pi\alpha} \left(\frac{J_0(kr)}{J_1(\alpha)} - \frac{J_0(\alpha)}{J_1(\alpha)} \right). \tag{3.11}$$

These monopoles cannot move, otherwise the centre of vorticity, which coincides with their own centre, would not be conserved (the proper momentum is $P' = 0$, so $R = 0$, according to (2.31)).

The two parameters $\alpha \equiv ka$ and Ω (or equivalently $\Gamma' = \Gamma - 2\pi a^2 \Omega$) are determined by (3.3) and (3.4). The relative circulation is

$$\Gamma' = 2\Gamma \frac{J_1(\alpha)}{J_3(\alpha)} \left(\frac{1}{2} - \frac{L}{\Gamma a^2} \right) \quad (3.12)$$

and the 'temperature' α satisfies an equation of state expressed in terms of the control parameter Υ and the scale radius $L/\Gamma a^2$ by

$$J_3^2(\alpha) = A^2 \left(\frac{2}{3} J_2^2(\alpha) - J_1(\alpha) J_3(\alpha) \right) \quad (3.13)$$

where

$$A = \left(\frac{3}{\mathcal{H}} \right)^{1/2} \left(\frac{1}{2} - \frac{L}{\Gamma a^2} \right) \quad (3.14)$$

with

$$\mathcal{H} = \Upsilon - \frac{3}{4} + \frac{L}{\Gamma a^2} - \frac{1}{2} \ln \left| \frac{L}{\Gamma a^2} \right|. \quad (3.15)$$

These results can be extended to positive temperatures by making the substitutions $k \rightarrow ik$, $\alpha \rightarrow i\alpha$ and using the identity $J_n(it) = i^n I_n(t)$ where $I_n(t)$ is the modified Bessel function of order n .

3.3. Rotating and translating dipoles

The dipole solutions can be written as a linear combination of a pure monopole term $J_0(kr)$ and a pure dipole term $J_1(kr) \sin \theta$, as

$$\psi' = \langle \psi' \rangle \left(1 - \frac{J_0(k_{1m}r)}{J_0(\alpha_{1m})} \right) - \frac{P'}{\pi a \alpha_{1m}} \frac{J_1(k_{1m}r)}{J_0(\alpha_{1m})} \sin \theta. \quad (3.16)$$

The boundary condition $\psi'(a) = 0$ can be only satisfied if the 'temperature' α is a zero α_{1m} of the Bessel function J_1 . On the other hand, the matching condition (3.9) determines the rotation rate by

$$\Omega = \frac{\Gamma}{2\pi a^2}. \quad (3.17)$$

When $\Gamma \neq 0$, the dipoles are asymmetric and rotate around the centre of vorticity with angular velocity Ω . The radius of rotation $R = -P'/\Gamma$ and the degree of asymmetry $\langle \psi' \rangle$ satisfy the equations of state, deduced from (3.3) and (3.4):

$$\frac{L}{\Gamma a^2} = -\frac{4\pi}{\Gamma} \langle \psi' \rangle + \frac{1}{2} - \left(\frac{R}{a} \right)^2, \quad (3.18)$$

$$\Upsilon = \frac{2\pi^2}{\Gamma^2} \alpha_{1m}^2 \langle \psi' \rangle^2 + \frac{3}{2} \left(\frac{R}{a} \right)^2 + \frac{2\pi}{\Gamma} \langle \psi' \rangle - \frac{L}{2\Gamma a^2} + \frac{1}{2} \ln \left| \frac{L}{\Gamma a^2} \right| + \frac{1}{2} \quad (3.19)$$

involving once again the control parameter Υ and the scale radius $L/\Gamma a^2$.

When $\Gamma \rightarrow 0$ (with ΓL finite), the radius of rotation $R \rightarrow \infty$ and we get a translating dipole ($\Omega = 0$) with travelling velocity $V = -\Omega R$ (see §2.4). Its angular momentum is infinite (since the centre of vorticity is rejected to infinity) but its linear impulse P is now independent of the origin and can serve as a control parameter.

Combining (3.17) and (2.31), we obtain

$$V = \frac{P}{2\pi a^2}. \quad (3.20)$$

This is of the general form (2.27) and we establish $C_{\mathcal{D}} = 2$ for a circular domain. The translating dipoles with discontinuous vorticity are still asymmetric due to the presence of the monopole term. Schematically, the monopole is ‘carried’ by the dipole and is called a *rider* (see figure 5*b*). Its amplitude $\langle\psi'\rangle$ is determined by (3.18) and (3.19), when $\Gamma \rightarrow 0$. Equation (3.18) returns (2.36) while (3.19) reduces to

$$E = \frac{1}{2}\pi\alpha_{1m}^2\langle\psi'\rangle^2 + \frac{P^2}{2\pi a^2}. \quad (3.21)$$

Of course, assuming $\Gamma = 0$ from the beginning would have led (more directly) to the same results, but, for the unity of the discussion, it is more convenient to treat a translating dipole as a rotating dipole with an infinite radius of rotation.

3.4. Classification of the stable isolated vortices

The previous solutions only cancel the first variations of the entropy (they are critical points). The analysis of the second variations will discard a lot of these solutions as no entropy maxima. This analysis is performed in §3.5 and gives the following results: (i) the stability to vorticity rearrangement at fixed boundary can be only satisfied if $\beta \geq \beta_{11}$ (where $\beta_{11} = -\pi\alpha_{11}^2 \simeq -46.12$ is the temperature of the fundamental dipole). If $\beta < \beta_{11}$, a quadrupolar perturbation is found to destabilize the vortex. (ii) The stability to boundary deformation demands $\beta \leq 0$ and, in most cases, $\overline{\omega}(a) \simeq 0$. In this section, we will consider that the stability conditions are exactly

$$\beta_{11} \leq \beta \leq 0, \quad (3.22)$$

$$\overline{\omega}(a) = 0. \quad (3.23)$$

A more accurate discussion is postponed to §3.5.

The condition of continuity (3.23) can be satisfied only if the vortex has a very specific radius. Therefore, its size which was a free parameter in the problem is in fact determined by the stability conditions (accounting for boundary deformation). As a result, we obtain a complete prediction of the equilibrium states in terms of the single control parameter Y (and the sign of ΓL).

The radius and the temperature of the monopoles (3.11) with continuous vorticity are determined by the equations of state

$$\frac{L}{\Gamma a^2} = \frac{1}{2} - \frac{J_3(\alpha)}{\alpha J_2(\alpha)}, \quad (3.24)$$

$$Y = \frac{1}{4} + \frac{J_3(\alpha)}{\alpha J_2(\alpha)} + \frac{2}{\alpha^2} \left(1 - \frac{3J_1(\alpha)J_3(\alpha)}{2J_2^2(\alpha)} \right) + \frac{1}{2} \ln \left| \frac{1}{2} - \frac{J_3(\alpha)}{\alpha J_2(\alpha)} \right| \quad (3.25)$$

resulting from (3.13)–(3.15). In figure 2, we have plotted the scaled radius (3.24) as a function of Y (dashed line). When $\Gamma L \leq 0$, the monopoles are always unstable. When $\Gamma L \geq 0$, the stable monopoles exist only in the range $Y_m \leq Y \leq Y_M$: below $Y_m = \frac{11}{24} - \frac{1}{2} \ln 3 \simeq -0.09097$ (obtained from (3.25) with $\alpha = 0$) the temperature is positive and above $Y_M = \frac{6}{\alpha_{11}^2} + \frac{1}{4} + \frac{1}{2} \ln \left| \frac{1}{2} - \frac{4}{\alpha_{11}^2} \right| \simeq -0.08151$ (obtained from (3.25) with $\alpha = \alpha_{11} \simeq 3.83$) the temperature is smaller than β_{11} , violating the stability condition (3.22). It is noteworthy that the range of stability is very narrow while the

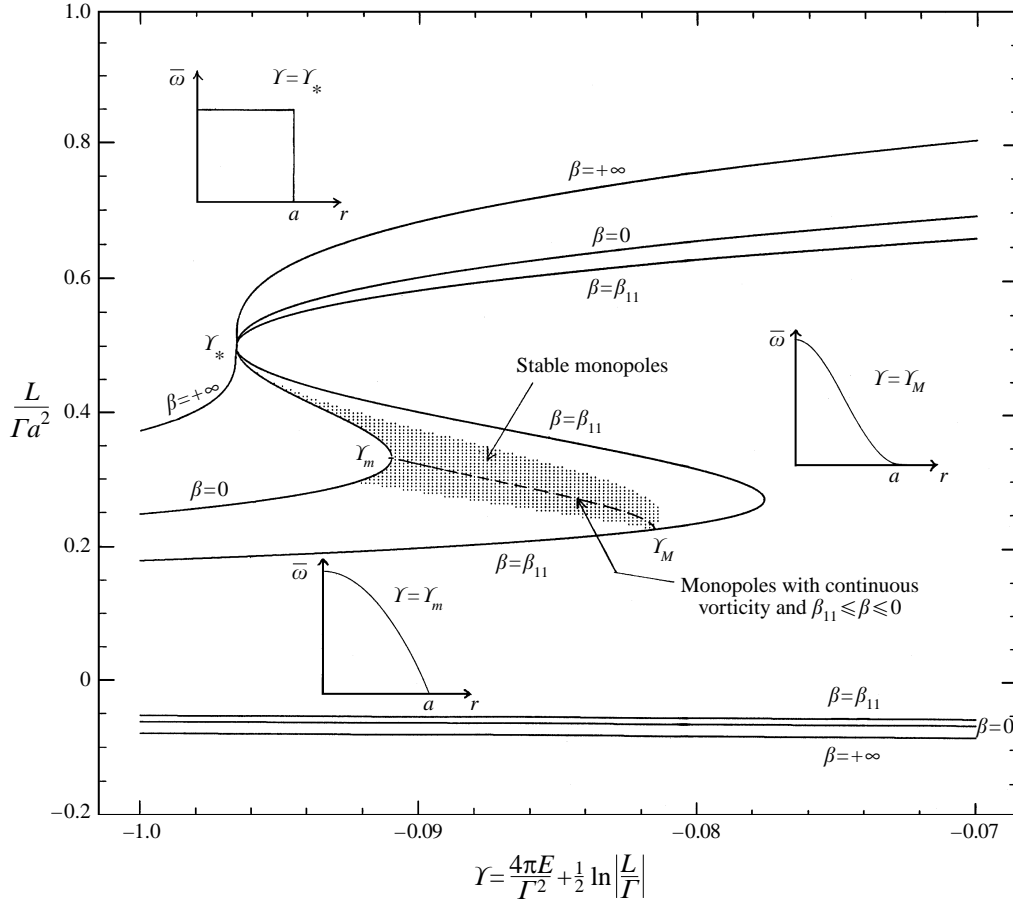


FIGURE 2. Stability diagram for the monopoles. The stable monopoles lie in the narrow grey region bordering the branch of monopoles with continuous vorticity and temperature $\beta_{11} < \beta < 0$ (dashed line). Their radius (the ordinate) is determined well by the single control parameter Y (the abscissa) and the scale factor L/Γ . Notice that the stable monopoles can exist only for $\Gamma L > 0$. The domain delimited by solid lines corresponds to linear monopoles with temperature $\beta_{11} < \beta < +\infty$. It has been obtained numerically, but its structure can be understood by a graphical study of equations (3.13)–(3.15). Beyond the curves $\beta = +\infty$, there is no linear monopole.

curve determining the vortex radius is very flat. As a result, we predict a typical size $a \sim 2(L/\Gamma)^{1/2}$ for the vortex radius (see figure 2), whatever the control parameter Y in $[Y_m, Y_M]$.

Some vorticity profiles are represented in figure 2. They correspond to a stream function

$$\psi' = \frac{\Gamma}{\pi\alpha^2} \left(\frac{J_0(kr)}{J_2(\alpha)} - \frac{J_0(\alpha)}{J_2(\alpha)} \right) \quad (3.26)$$

obtained from (3.11), (3.12) and (3.24). The stable monopoles have similar profiles: the vorticity monotonically decreases with r (if $\Gamma > 0$) until $\bar{\omega} = 0$. The monopoles with an oscillating vorticity are always unstable. This property, compatible with linear stability analysis, results directly from (3.22): indeed, α_{11} is not only the first zero of Bessel function J_1 but it corresponds also to the first minimum of Bessel function J_0 (since $J_0'(t) = -J_1(t)$). For $Y = Y_m$, $\beta = 0$, $\Omega \rightarrow \infty$ and the vorticity has a parabolic

profile $\bar{\omega} = (2\Gamma/\pi a^2)(1 - r^2/a^2)$ (a limit case of (3.26) when $k \rightarrow 0$). For $Y = Y_M$, $\alpha = \alpha_{11}$ and the vorticity vanishes at the edge of the vortex with a horizontal slope.

The previous results are valid for $\Gamma \neq 0$. The monopoles with $\Gamma = 0$ and $L \neq 0$ correspond to a diverging control parameter ($Y \sim 4\pi E/\Gamma^2 \rightarrow +\infty$) and are therefore unstable (their temperature $\beta = \beta_{2m} = -\pi\alpha_{2m}^2$, determined by (3.25), is always smaller than β_{11}). The case $\Gamma = L = 0$ is very singular and cannot be easily obtained as a limit of the previous study. Coming back to equations (3.3), (3.4) and (3.11), we find $\beta = \beta_{3m} < \beta_{11}$ and $\bar{\omega}(a) \neq 0$ for any radius. As a result, the monopoles with zero circulation are always unstable in our case of a linear relationship between vorticity and stream function.†

We now consider the case of dipoles. As discussed in §3.3, the temperature of the dipoles is ‘quantized’: it must be a zero α_{1m} of the Bessel function J_1 . *A priori* m can be any integer, but the stability condition (3.22) selects only the fundamental mode $m = 1$. In addition, their vorticity must be continuous, according to (3.23). This is satisfied for a specific radius given by

$$\frac{L}{\Gamma a^2} = \tau_c - \tau, \quad (3.27)$$

$$Y = 1 + \frac{1}{2}\tau + \frac{3}{2}(\tau - \tau_c) + \frac{1}{2} \ln |\tau - \tau_c| \quad (3.28)$$

where $\tau \equiv (R/a)^2$ is a kind of aspect ratio and $\tau_c \equiv \frac{1}{2} - 4/\alpha_{11}^2 \simeq 0.22756$ is a shorthand notation. The degree of asymmetry is simply:

$$\langle \psi' \rangle = \frac{\Gamma}{\pi\alpha_{11}^2} \quad (3.29)$$

and the relative stream function (3.16) reduces to

$$\psi' = \frac{\Gamma}{\pi\alpha_{11}^2} \left(1 - \frac{J_0(k_{11}r)}{J_0(\alpha_{11})} \right) + \frac{\Gamma R}{\pi a \alpha_{11}} \frac{J_1(k_{11}r)}{J_0(\alpha_{11})} \sin \theta. \quad (3.30)$$

The equation of state (3.28) determining the aspect ratio τ has two branches of solutions (see figure 3). The upper branch with $\tau > \tau_c$ is only accessible when $\Gamma L < 0$, while the lower branch, with $\tau < \tau_c$, exists only for $\Gamma L > 0$ and $Y < Y_M$.

Let us consider some special limits: when $L \rightarrow 0$ (with $\Gamma \neq 0$), the control parameter Y diverges to $-\infty$ and the aspect ratio $\tau \rightarrow \tau_c$. Combining (3.27) and (3.28), we obtain $4\pi E/\Gamma^2 = 1 + \frac{1}{2}\tau_c - \ln a$ which determines the vortex radius a , and the radius of rotation $R = (a\tau_c)^{1/2}$. When $\Gamma \rightarrow 0$ and $L \rightarrow \infty$ (with $\Gamma L < 0$), the control parameter Y diverges to $+\infty$ and we get a translating dipole ($\tau \rightarrow \infty$). Since the vorticity is continuous, this dipole is symmetric (no rider) with relative stream function

$$\psi' = -\frac{P}{\pi a \alpha_{11}} \frac{J_1(k_{11}r)}{J_0(\alpha_{11})} \sin \theta. \quad (3.31)$$

Its radius is given by the relation

$$E = \frac{P^2}{2\pi a^2} \quad (3.32)$$

resulting from (2.36) and the asymptotics $Y \sim 4\pi E/\Gamma^2$, $\tau \sim \frac{1}{2}Y$, $L/\Gamma a^2 \sim -\tau$. This

† Note that robust monopoles with zero circulation have been observed in laboratory by Kloozterziel & van Heijst (1992), and linear stability has been shown for families of zero-circulation monopoles by Carton *et al.* (1989) and by Carton & Legras (1994). However, these stable monopoles are characterized by a nonlinear relationship between vorticity and stream function.

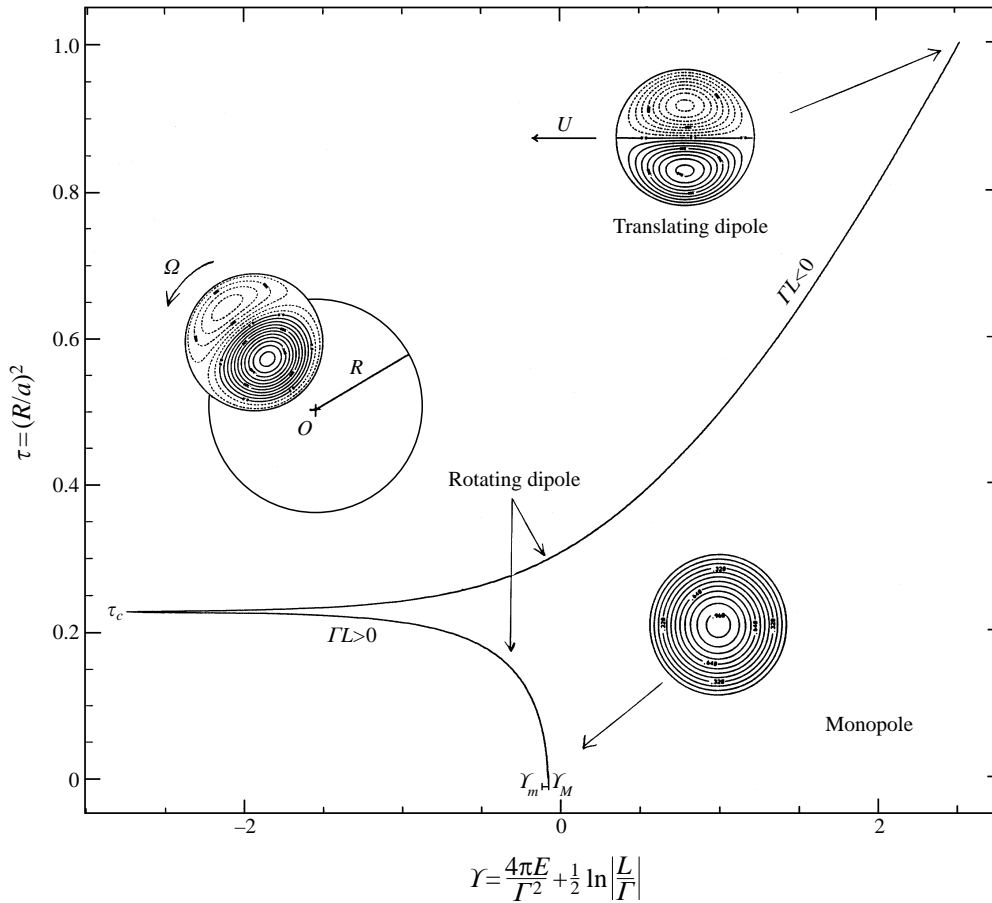


FIGURE 3. Recapitulatory diagram classifying the stable monopoles and dipoles (in translation or rotation) as a function of the single control parameter γ (and the sign of ΓL). The ordinate represents the aspect ratio of the rotating dipoles determined by the equation of state (3.28). The segment at $R = 0$ corresponds to monopoles (which do not move). Examples of vorticity fields are shown for illustration (solid lines are positive vorticity isovalues and dotted lines negative ones).

‘particle’ (called a *modon* in geophysics) travels with a velocity

$$V = E/P \quad (3.33)$$

obtained from (3.20) and (3.32).

These solutions, represented in figure 3, can be compared with the three kinds of structures found in a bounded domain by Chavanis & Sommeria (1996). The monopoles (3.26) exist at various temperatures given by the equation of state (3.25) and form what we called the *continuum* phase. In contrast, the translating dipole (3.31) is a *discrete* mode (the fundamental eigenfunction of the Laplacian with zero average) which can exist only at $\beta = \beta_{11}$ (the corresponding eigenvalue). These two solutions are connected by the rotating dipoles (3.30) which can be considered, in the language of phase transitions, as a *coexistence* between the two previous phases (since they correspond to a linear combination of solutions (3.26) and (3.31)). This coexistence is possible for $\beta = \beta_{11}$ only, like the coexistence of a liquid and a solid phase at the transition temperature. The proportion $\tau^{1/2} = R/a$ of these two phases is

determined by the control parameter Y via the equation of state (3.28). When $Y = Y_M$, we have $R = 0$ and we recover the standing monopole with temperature β_{11} . When both phases coexist, one lobe of the dipole dominates the other and the structure rotates. Finally, when $Y \rightarrow +\infty$, the two lobes have equal strength, the radius of rotation R becomes infinite and the dipole translates.

For $Y_m < Y < Y_M$ (and $\Gamma L > 0$), monopolar and dipolar structures are predicted (with different radius). We could try to compare their entropy to decide which structure will be selected at equilibrium; however, both structures are local maxima of entropy and it is more plausible that the selection will be made by the relaxation process and the topology of the initial condition (rather than the pure comparison of their entropy).

Tripoles are never selected as stable structures in the bounded disk (in the linearized approximation). Similarly, the stability condition (3.22), stating $\beta \geq \beta_{11}$, would exclude tripoles as well as all higher-order structures (which involve larger eigenvalues) in the linearized limit. However, this is only a suggestion here, as their shape is not a disk and we do not have explicit solutions for them.

Finally, we must not forget that the domain (\mathcal{D}) is necessarily larger than the domain (\mathcal{D}_0), initially containing the non-zero vorticity. With our non-dimensional units $|\mathcal{D}_0| = 1$, so that this condition imposes $\pi a^2 > 1$, or equivalently

$$\pi \left| \frac{L}{\Gamma} \right| > \left| \frac{L}{\Gamma a^2} \right|. \quad (3.34)$$

This leads to a further restriction on the stable states. For instance, the monopoles are only obtained for $L/\Gamma a^2 > 0.227$ (reached for $Y = Y_M$, see figure 2), and due to (3.34), this is only possible if $L/\Gamma > 0.0723$. In the case of a translating dipole, the radius is given by (3.32) and the same condition $\pi a^2 > 1$ implies $P^2/2E > 1$: there is no possible equilibrium in a single structure if the momentum is too small. We then expect a splitting into several bubbles, as observed in some numerical computations.

3.5. Selection by maximum entropy

We derive here the conditions of stability (3.22), (3.23) used in §3.4, starting from the general expressions given in §2.5. In the linearized limit, we can simplify these expressions considerably and find some destabilizing perturbations which discard many solutions as not entropy maxima.

First of all, we show that the condition of stability to vorticity rearrangement in a fixed domain (\mathcal{D}) discards the solutions which have a temperature β smaller than the temperature β_{11} of the fundamental dipole (or equivalently $\alpha > \alpha_{11} \simeq 3.83$, the first zero of Bessel function J_1).

To that purpose, we choose a particular perturbation $\delta\rho(\mathbf{r}, \sigma)$ and calculate the corresponding second variations (2.37) of the free energy. Such a perturbation depends both on the position \mathbf{r} and on the distribution of the vorticity levels σ . However, we can choose only the dependence on position $\delta\bar{\omega}(\mathbf{r})$ and find the most destabilizing distribution of vorticity levels by an optimization calculation. In the limit of strong mixing, the equilibrium probability is almost uniform $\rho(\mathbf{r}, \sigma) \simeq \gamma_{\mathcal{D}}(\sigma)/\pi a^2$ (see Chavanis & Sommeria 1996), so that the second variations of the entropy (the first term in (2.37)) are locally proportional to $\delta^2 s = -\int ((\delta\rho)^2/\gamma_{\mathcal{D}}(\sigma))d\sigma$. The perturbation $\delta\rho$ must satisfy the normalization condition (2.1) to first order $\int \delta\rho d\sigma = 0$, and for a given perturbation $\delta\bar{\omega}$, we must have also $\int \delta\rho \sigma d\sigma = \delta\bar{\omega}$. We can easily show that the most destabilizing perturbation (which maximizes $\delta^2 s$ with the two previous

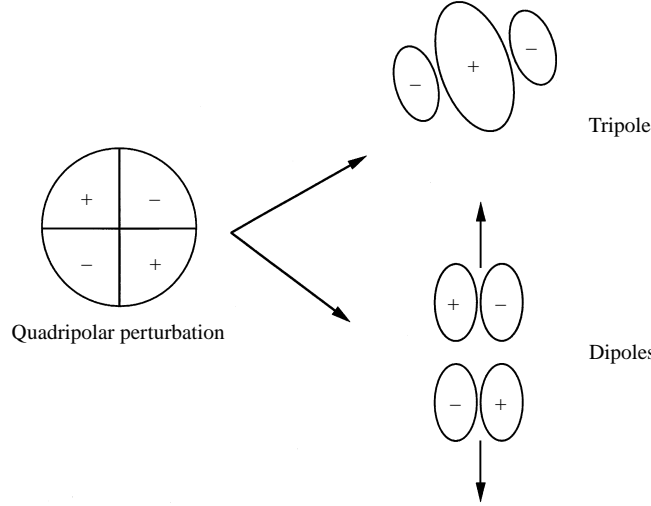


FIGURE 4. Schematic evolution of a monopole destabilized by a quadrupolar perturbation of the form (3.37). The vortex could further evolve towards a tripole or break down into two dipoles translating in opposite directions.

constraints) is

$$\delta\rho(\mathbf{r}, \sigma) = \left(\sigma - \frac{\Gamma}{\pi a^2} \right) \gamma_{\mathcal{D}}(\sigma) \delta\bar{\omega}(\mathbf{r}). \quad (3.35)$$

The second variations (2.37) of the free energy are therefore always smaller than

$$\delta^2 J = -\frac{\pi a^2}{2} \int (\delta\bar{\omega})^2 d^2\mathbf{r} - \frac{1}{2}\beta \int \delta\psi \delta\bar{\omega} d^2\mathbf{r}. \quad (3.36)$$

Let us now consider a quadrupolar perturbation of the form

$$\delta\bar{\omega}(\mathbf{r}) = J_2(k_{11}r) \sin 2\theta \quad (3.37)$$

with $k_{11} = \alpha_{11}/a$. The associated stream function compatible with the boundary conditions (continuity of the stream function and of the velocity) is $\delta\psi = \delta\bar{\omega}/k_{11}^2$ (inside the subdomain \mathcal{D}). Moreover, it can be readily verified that (3.37) conserves the constraints to first order. Indeed it does not change the circulation nor the angular momentum, because of its zero angular mean. The impulse is also unchanged by this quadrupolar perturbation, unlike for the dipolar perturbation (proportional to $\sin\theta$) considered in a bounded domain by Chavanis & Sommeria (1996). Finally, the basic state is either a monopole (3.11) or a dipole (3.16), so it is orthogonal to the perturbation, and the energy constraint is satisfied to first order.

The second variations (3.36) of the free energy induced by this perturbation are proportional to

$$\delta^2 J = \frac{\pi^2 a^4}{2} \left(\frac{\beta}{\beta_{11}} - 1 \right). \quad (3.38)$$

They are strictly positive when $\beta < \beta_{11}$. Therefore, when $\beta < \beta_{11}$, the critical point (3.11) cannot be a local entropy maximum: we can figure out that the quadrupolar perturbation will grow. The monopole will presumably break down into two dipoles translating in opposite directions, or form a tripole (see figure 4) like in the experiments of Kloosterziel & van Heijst (1991) or in the numerical simulations of Carton &

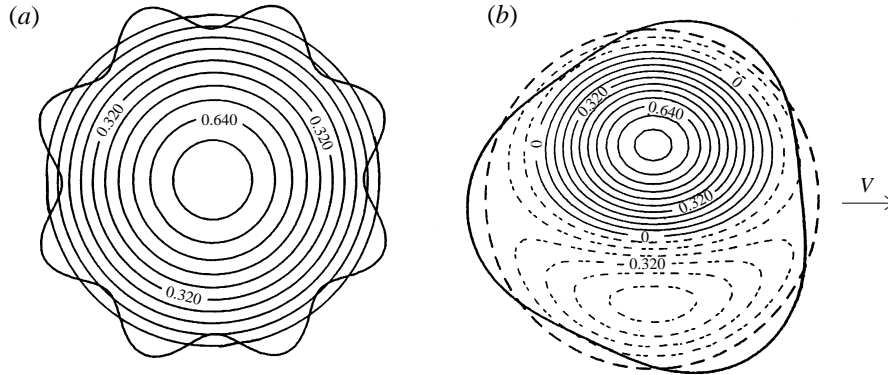


FIGURE 5. Boundary deformation of a monopole (a) and of a dipole (b) corresponding to formulae (3.40) and (3.46). The deformation (3.46) tends to evacuate some vorticity behind the dipole; this is consistent with the trail observed in laboratory experiments and numerical simulations. The particular dipole represented on (b) is translating ($\Gamma = 0$) and carries a ‘rider’ (see § 3.3). Its vorticity field, proportional to $\bar{\omega} = \lambda J_0(k_{11}r) + J_1(k_{11}r) \sin \theta$ with $\lambda = (2\pi a^2 E/P^2 - 1)^{1/2}$, is discontinuous at $r = a$ (except in the symmetric case $\lambda = 0$). The second variations (3.47) of the free energy induced by the deformation (3.46) are proportional to $\delta^2 J_d = \lambda^2 - \frac{3}{16} J_3(\alpha_{11}) J_5(\alpha_{11}) / J_4^2(\alpha_{11}) \simeq \lambda^2 - 0.13$: for stability reasons, the amplitude of the rider must be less than $\lambda_c \simeq 0.36$. The dipole of (b), corresponding to $\lambda = 0.5$ is therefore unstable.

Legras (1994) and Robert & Rosier (1997). The same criterion $\beta < \beta_{11}$ eliminates higher-order dipolar solutions (3.16), with temperature $\beta = \beta_{1m}$ when $m > 1$.

We now show that the condition of maximum entropy when we deform slightly the boundary of the subdomain (\mathcal{D}) implies that the temperature must be negative and that, in most cases, the vorticity must be continuous (or slightly discontinuous) across ($\partial\mathcal{D}$).

In the case of monopoles (3.11), we consider a perturbation of the form

$$\lambda(r, \theta) = J_m(kr) \sin(m\theta) \quad (3.39)$$

where k is the wavenumber of the monopole that we want to perturb. We show in Appendix B that λ can be associated with an incompressible velocity field of deformation \mathbf{U} which satisfies the constraints to first order if $m > 1$. The deformation of the boundary corresponding to this perturbation (represented in figure 5a) is given by (2.50), yielding

$$U_r(a, \theta) = -\frac{2\pi a^3}{\Gamma' \alpha^2} J_m(\alpha) \sin(m\theta). \quad (3.40)$$

The second variations of the free energy (2.51) are obtained by solving the problem (2.46). When $\tilde{\beta} < 0$, we find in Appendix B

$$\delta^2 J_d = \frac{\tilde{\beta} \pi a^4}{2m\alpha^2} \left(J_{m-1}(\alpha) - \bar{\omega}(a) \frac{2\pi a^2 J_m(\alpha)}{\Gamma' \alpha} \right) \left(J_{m+1}(\alpha) + \bar{\omega}(a) \frac{2\pi a^2 J_m(\alpha)}{\Gamma' \alpha} \right). \quad (3.41)$$

These results can be easily extended to positive temperatures with the aid of modified Bessel functions (see § 3.2). We can obtain interesting results by considering special limits of expression (3.41). If the discontinuity $\bar{\omega}(a)$ of the vorticity is strong (and α not too small), equation (3.41) simplifies to

$$\delta^2 J_d \simeq -\frac{2\tilde{\beta} \pi^3 a^8}{m\Gamma'^2 \alpha^4} J_m^2(\alpha) \bar{\omega}(a)^2 > 0 \quad (3.42)$$

which is strictly positive (since $\tilde{\beta} < 0$). As a result, when the vorticity is strongly discontinuous, the vortex is not stable with respect to boundary deformations.

The deformation criterion also makes a clear distinction between positive and negative temperatures. Let us consider the case of a continuous vorticity $\overline{\omega}(a) = 0$; then, the second-order variation of the free energy (3.41) valid for negative temperatures becomes

$$\delta^2 J_d = \frac{\tilde{\beta} \pi a^4}{2m\alpha^2} J_{m-1}(\alpha) J_{m+1}(\alpha). \quad (3.43)$$

Since $m > 1$ and $\alpha < \alpha_{11}$, we have $\delta^2 J_d \leq 0$: the monopoles with a continuous vorticity and a negative temperature are stable with respect to boundary deformation. In contrast, in the case of positive temperatures, we find

$$\delta^2 J_d = (-1)^{m+1} \frac{\tilde{\beta} \pi a^4}{2m\alpha^2} I_{m-1}(\alpha) I_{m+1}(\alpha). \quad (3.44)$$

When m is odd, $\delta^2 J_d > 0$: the monopoles with positive temperatures are unstable. This result has been obtained for a continuous vorticity but it remains valid in any case, as seen by a systematic determination of the variations (3.41) for different modes $m = 2$ to 10 (it turns out that higher modes do not bring new possibilities of instability). For this purpose, we scan the two parameters Y and $L/\Gamma a^2$, determine the corresponding values of α , Γ' , $\overline{\omega}(a)$ from (3.11)–(3.15) and calculate $\delta^2 J_d$ from (3.41). We have limited our analysis to the part of the plane (delimited by solid lines) inside which $\beta > \beta_{11}$ (outside this region, the stability condition corresponding to (2.37) is not satisfied). We then observe that the stable vortices ($\delta^2 J_d < 0$) lie in a very narrow region (in grey in figure 2) bordering the line of the monopoles with a continuous vorticity and a negative temperature (the dashed line). As a result, the stability criteria bring very strong constraints on the possible size of the equilibrium vortex; from figure 2, we can estimate that the statistical theory allows only a deviation of order 10% (in radius) with the continuous monopole. There is also a region of stability for $Y \leq Y_m$. It corresponds to monopoles with discontinuous vorticity and slightly negative inverse temperatures. The discontinuity $\overline{\omega}(a)$ increases monotonically when we vary the control parameter from Y_m to Y_* . At $Y_* = \frac{1}{4} - \frac{1}{2} \ln 2 \simeq -0.0966$, the discontinuity is maximum and we obtain a disk of radius $L/\Gamma a^2 = \frac{1}{2}$.

In the case of dipoles, we consider a perturbation of the form

$$\lambda(r, \theta) = J_4(k_{11}r) \sin(4\theta) + \eta J_1(k_{11}r) \cos \theta \quad (3.45)$$

where k_{11} is the wavenumber of the unperturbed dipole (3.16). The first term in (3.45) does not satisfy the conservation of the impulse P_y ; to restore it, we have added a solid rotation (corresponding to the second term). The coefficient η is adjusted in order to have exactly $\delta P_y = 0$ (see Appendix B). The first term of this perturbation is in a mode $m = 4$, yielding a boundary deformation (2.50) of the form

$$U_r(a, \theta) = -\frac{2\pi a^4}{P' \alpha_{11}^2} J_4(\alpha_{11}) (\cos \theta + \cos 3\theta). \quad (3.46)$$

This is the first non-trivial deformation we can choose: the mode $m = 2$ yields only the term in $\cos \theta$ corresponding to a pure translation (so it does not change the free energy) and the mode $m = 3$ has not the right symmetry to be associated with an incompressible velocity field of deformation. In contrast, as shown in Appendix B, the mode $m = 4$ satisfies this condition and also satisfies the integral constraints to first order (when superimposed on a solid rotation η). Moreover, the deformation

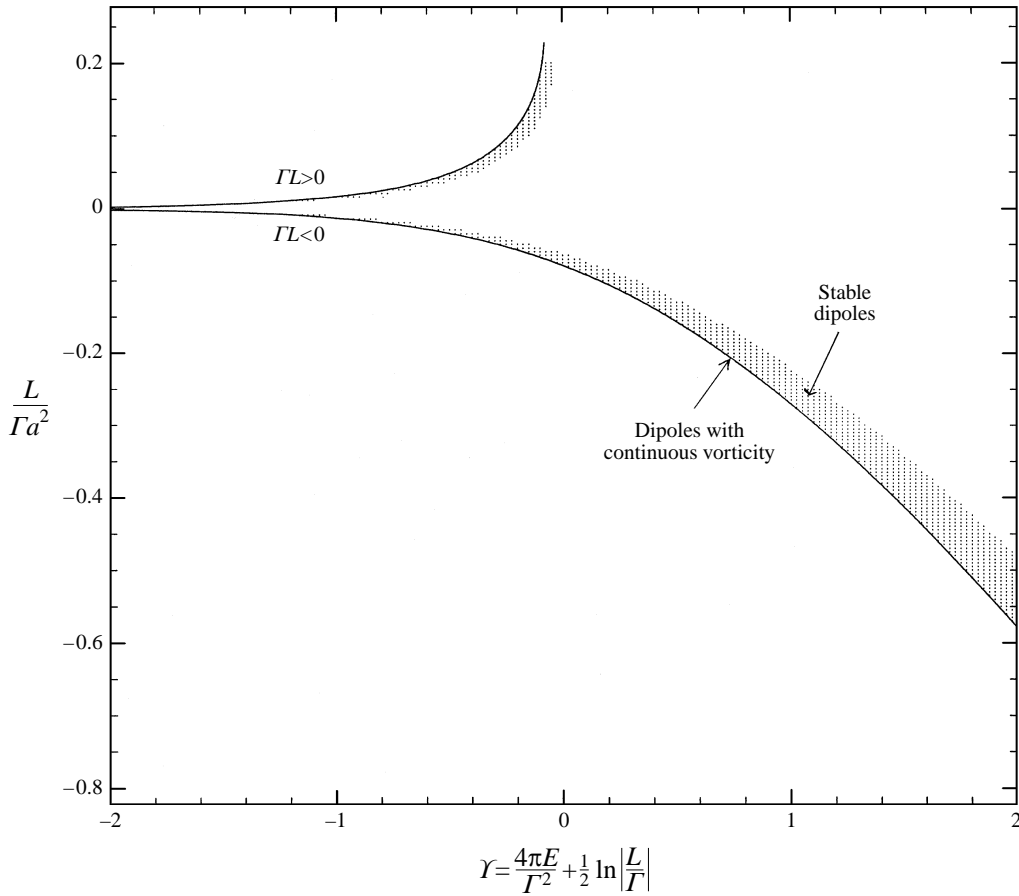


FIGURE 6. Stability diagram for the dipoles. The stable dipoles lie in the narrow grey regions bordering the branch of dipoles with continuous vorticity (solid lines). Their radius (the ordinate) is well determined by the single control parameter Υ (the abscissa) and the scale factor L/Γ . Linear dipoles are only possible in the domain enclosed by the solid lines.

in $\cos 3\theta$ represented in figure 5(b) tends to create a trail behind the dipole which is often observed in numerical simulations and laboratory experiments (see e.g. van Heijst & Flor 1989).

This perturbation has therefore a nice structure. The second-order variations of the free energy (2.51) are (see Appendix B)

$$\delta^2 J_d = -\frac{\tilde{\beta}_{11}\pi a^4}{8\alpha_{11}^2} \left(\frac{16\pi^2 a^6}{3P'^2 \alpha_{11}^2} J_4^2(\alpha_{11}) \overline{\omega}(a)^2 - J_3(\alpha_{11}) J_5(\alpha_{11}) \right). \quad (3.47)$$

When the vorticity is strongly discontinuous, the first term dominates and $\delta^2 J_d > 0$; in contrast, for weak discontinuities, only the second term remains and $\delta^2 J_d < 0$. As before, we find that the condition of maximum entropy with respect to boundary deformation forbids a strong discontinuity of vorticity. To be more precise, we have represented the stability diagram of the dipoles in figure 6. We can first notice that the equation of state (3.18), (3.19) has solutions only in the domain enclosed by the solid curves. We can easily verify that these curves correspond to the dipoles with a continuous vorticity. As a result, the continuous dipole is the smallest dipole we can

construct (in the linearized limit) for a given set of control parameters. Dipoles with higher radii exist but they are more and more discontinuous and must be rejected as not entropy maxima via boundary deformation. Once again, we observe that this stability condition is very stringent since the stable solutions (satisfying $\delta^2 J_d < 0$) lie in a very narrow range (in grey) near the continuous dipoles. From figure 3, or by direct calculation, we can estimate that the deviation from the continuous dipole must be less than 10% (in radius) and is even smaller when $Y \rightarrow -\infty$.

4. Comparison with a minimum-entropy principle

A first attempt to predict the organization into an isolated vortex by an optimum principle was made by Leith (1982). His theory is based on a selective decay hypothesis (see e.g. Kraichnan & Montgomery 1980) for two-dimensional slightly viscous flows: the system organizes into a minimum-entropy state with given ‘rugged’ conserved quantities such as energy, circulation and angular momentum. It predicts a linear relationship between vorticity and stream function and an optimal radius which provides a continuous vorticity at the edge of the vortex. We found that his theory must be improved to avoid possible inconsistencies.

(i) Leith restricts the problem to axisymmetric structures (which is always possible) but he also constrains the perturbations to be axisymmetric; this is an artificial limitation because non-axisymmetric perturbations are more destabilizing than axisymmetric ones. For example, a monopole with zero circulation is stable under axisymmetric perturbations but unstable under non-axisymmetric perturbations. This was observed by Leith through numerical experiments (leading to the formation of a tripole) as he mentions in the conclusion of his article, but this was not predicted by his theoretical work.

(ii) He considers very particular control parameters: his so-called MEV M corresponds to a vortex with zero circulation ($\Gamma = 0$) and his MEV C has no angular velocity ($\Omega = 0$). This limitation is not necessary and in Appendix C, we generalize his results to arbitrary values of the control parameters.

(iii) Finally, there is another, more fundamental, difficulty: Leith minimizes the entropy G with respect to the radius and finds an optimal radius by the condition $\delta G = 0$ which happens to correspond to a vorticity continuously dropping to zero at the vortex edge. However, it turns out that this is just an inflection point of G versus radius ($\delta^2 G = 0$), as shown in figure 7. In fact the entropy decreases monotonically with the radius and there is no minimum, so the variational condition is not truly satisfied.

Our analysis avoids these inconsistencies by introducing the concept of a ‘maximum entropy bubble’. The restriction to a subdomain is justified by kinetic processes and the size of the structure results from stability conditions: it is only for a narrow range of radii, corresponding to a nearly continuous vorticity, that the structure is stable to boundary deformations. Moreover, in the limit of strong mixing, we can show that a ‘maximum-entropy bubble’ is equivalent to a ‘minimum-entropy bubble’. Indeed, minimizing entropy at fixed boundary ($\partial \mathcal{D}$) yields a linear relationship between vorticity and stream function, like in the limit of strong mixing of the statistical theory. Moreover, in this limit, we can relate the entropy at equilibrium to the coarse-grained entropy by the relationship (see Chavanis & Sommeria 1996)

$$|\mathcal{D}| \Gamma_2^{\text{c.g.}} = \Gamma^2 - 2\mathcal{S} \quad (4.1)$$

which clearly shows an equivalence between a maximum-entropy state and a minimum-

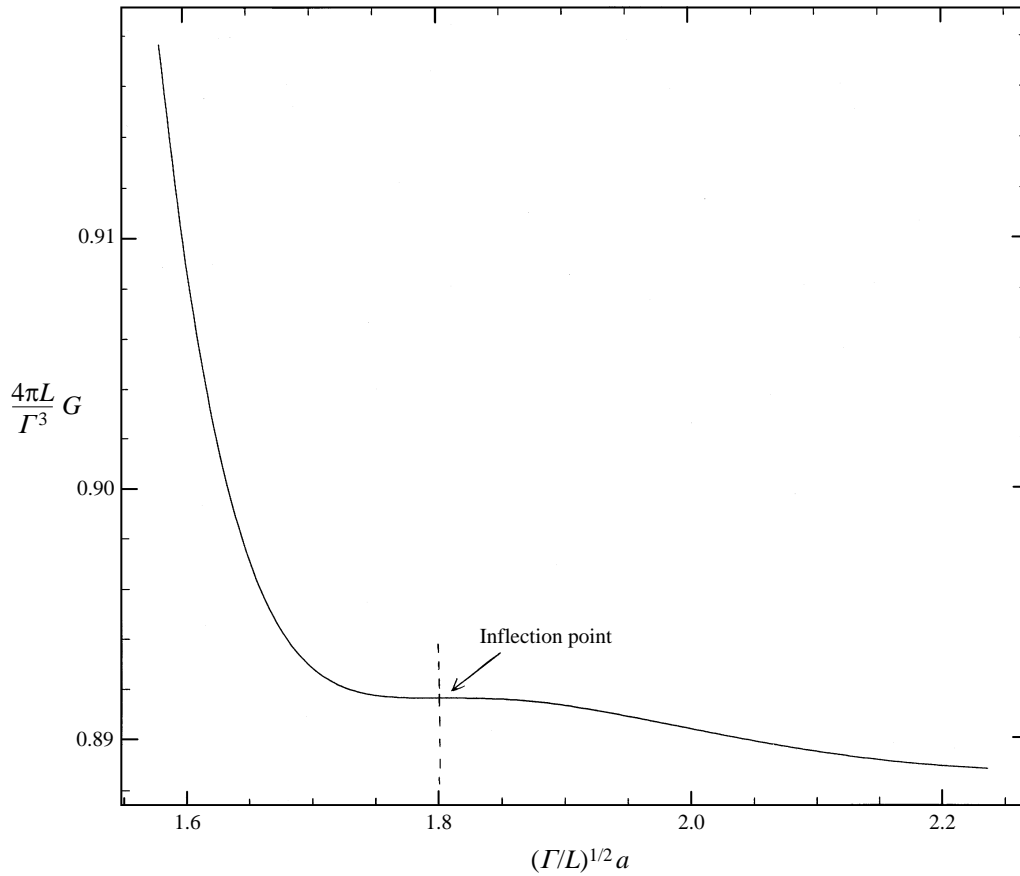


FIGURE 7. Enstrophy vs. radius for linear vortices. The critical point of this curve corresponds to a monopole with continuous vorticity. The control parameter is equal to $\Upsilon \simeq -0.08828$. According to (C 16) and (C 17) (with $m = 1$), this monopole corresponds to Leith's MEV C ($\Omega = 0$) with radius $(\Gamma/L)^{1/2}a \simeq 1.8009$. This vortex is not a local minimum of enstrophy (versus radius) but rather an inflection point.

enstrophy state in a given subdomain (we have introduced the notation $\mathcal{S} \equiv (1 - (\Gamma^2/|\mathcal{D}|))(S - S_0)$, where S_0 is the entropy corresponding to uniform density probabilities).

To be more complete, we can compare the second variations of the two functionals $\Gamma_2^{\text{c.g.}}$ and S around equilibrium. The second variations of the enstrophy $\delta^2 \Gamma_2^{\text{c.g.}} = \frac{1}{2} \int (\delta \bar{\omega})^2 d^2 \mathbf{r}_o$ depend only on the perturbation $\delta \bar{\omega}$ of the locally averaged vorticity field, while the second variations of the entropy $\delta^2 S = -\frac{1}{2} \int ((\delta \rho)^2 / \rho) d^2 \mathbf{r}_o d\sigma$ depend on the optimal density probability ρ and on the perturbation $\delta \rho$ of the density probability around this optimal state. However, we have shown in § 3.5 that, in the limit of strong mixing, we could make the approximation $\rho(\mathbf{r}_o, \sigma) \simeq \gamma_{\mathcal{D}}(\sigma) / |\mathcal{D}|$ and that the most destabilizing perturbations were of the form $\delta \rho(\mathbf{r}_o, \sigma) \propto \gamma_{\mathcal{D}}(\sigma)(\sigma - \Gamma/|\mathcal{D}|)\delta \bar{\omega}(\mathbf{r}_o)$. Then, the second variations of the entropy are proportional to $\delta^2 S = -\frac{1}{2} \int (\delta \bar{\omega})^2 d^2 \mathbf{r}_o$ like the second variations of the enstrophy (with the opposite sign). Finally, the stability conditions to boundary deformation are the same in each case because we just displace the vorticity without changing entropy or enstrophy. Therefore, a

minimum-entropy state is completely equivalent to a maximum-entropy state in the limit of strong mixing when we introduce the concept of an ‘optimal bubble’.

5. Discussion and conclusions

We have proposed a general explanation for the self-organization of two-dimensional turbulence into isolated vorticity structures. Such structures emerge as statistical equilibrium states of the Euler equation, provided we make the additional assumption of a maximum-entropy bubble: vorticity mixing is restricted to a domain with a given area, but deformable shape. This structure depends only on the conserved quantities, and on the area of this bubble. The latter depends on kinetic constraints, but it appears that equilibrium solutions can be obtained only for a very restricted range of areas, so that this area can be predicted within a good approximation from the conserved quantities only.

The equilibrium states can be obtained in principle as solutions of the well-defined variational problem stated in §2, but the practical resolution of this free boundary problem will require the development of appropriate numerical methods. We make, however, some general predictions (in §2) without actually solving the variational problem. In particular, self-organization always results in a steadily translating or steadily rotating structure (or possibly into several separated structures) characterized by a monotonic† relationship between vorticity and stream function.

Moreover, we can get a good idea of the general equilibrium solutions by assuming a linear relationship between vorticity and stream function. This is justified as a particular limit of strong mixing, discussed by Chavanis & Sommeria (1996) for a bounded domain. In this limit, the maximum-entropy principle is equivalent to a minimum-entropy principle, stated in §4 and compared with the minimum entropy principle used by Leith (1984). Notice that these two principles are not identical: in both cases, entropy is minimized with respect to internal vorticity rearrangements, but Leith (1984) also minimizes the entropy with respect to variations of the vortex radius a (in fact, this does not give a true minimum but an inflection point), while we minimize entropy with respect to boundary deformations with a fixed area. Furthermore Leith restricts his analysis to axisymmetric equilibria with particular values of the conserved quantities, and considers only axisymmetric perturbations. Our analysis is much more general.

We have shown in §3 that the vorticity structures with a linear relationship between vorticity and stream function only depend on a parameter γ and on a scaled radius $a|\Gamma/L|^{1/2}$. The control parameter γ is constructed from the energy E , circulation Γ and angular momentum L . This analysis therefore provides a monopole and a dipole solution for any set of conserved quantities and any radius a (restricted to an appropriate domain of existence for solutions, as indicated in figures 2 and 6). This is an interesting result, even without reference to the underlying statistical theory. Indeed, although these monopole and dipole vorticity fields are well-known solutions of the Euler equation, their determination for a given set of conserved quantities is a nonlinear problem (due to the nonlinear energy constraint), and it is not straightforward.

The condition of a local entropy maximum, obtained by analysing the second variations, considerably restricts this set of solutions: the grey areas in figures 2 and

† It must be an increasing function, corresponding to a negative temperature β , in the linearized case, and it is probably true more generally for any isolated equilibrium vorticity structure.

6 indicate the ranges of parameters leading to such stable solutions. These are in a small neighbourhood of the lines corresponding to solutions with a continuously vanishing vorticity at the vortex boundary. This condition of continuity determines the vortex radius as a function of the single control parameter Υ (and the sign of ΓL). As a result, we obtain a nice classification of isolated structures in terms of this single control parameter, as shown in figure 3. Depending on this parameter, we predict monopole or dipole structures (rotating or translating) and our classification gives a unified picture of the ‘zoology’ of coherent structures. We were not able to look for tripole solutions, as the boundary is not a circle, but we argue in §3.4 that they are probably unstable in the linearized limit, as well as all higher-order structures (quadrupoles etc). Tripoles are, however, obtained as a restricted statistical equilibrium far from the limit of strong mixing, as shown numerically by Robert & Rosier (1997).

The selection of the radius can be physically interpreted as follows: if the radius of the mixed region (i.e. the vorticity structure) is below the narrow range of stability, its contour will deform more and more, as this deformation brings free energy to the system, which allows the entropy to increase by internal rearrangement. This deformation should occur until it irreversibly entrains surrounding fluid in the mixed region, which then reaches a larger radius. If the radius is instead beyond the range of stability, we expect that the contour deforms until it splits in two (or more) separate structures. In §3.5, we have examined the free energy brought by different modes of perturbation, and this provides hints for likely modes of instability. For instance, in the case of a dipole, the mode of deformation shown in figure 5*b* can grow when the radius is too large (beyond the grey areas of figure 6), corresponding to an excessive discontinuity of the vorticity at the dipole boundary. As this perturbation further develops, we anticipate that vorticity will be released behind the dipole, and this process is indeed commonly observed in numerical simulations or laboratory experiments. We have found also that monopoles with positive and negative vorticity are always unstable: the quadrupolar internal perturbation sketched in figure 4 will increase the entropy. The further development of this perturbation would correspond to the formation of a tripole, or to the splitting into two dipoles, and this is indeed observed in the laboratory experiments of Kloosterziel & van Heijst (1991) and in the numerical simulations of Carton & Legras (1994) and Robert & Rosier (1997).

From the curves of figure 3, we can predict a final state resulting from arbitrary initial conditions, by calculating the corresponding conserved quantities contributing to the control parameter Υ . Monopoles are predicted in the small interval $[\Upsilon_m, \Upsilon_M]$ if $\Gamma L > 0$. Dipoles are also possible for the same range of parameters, but with a different radius, and the choice will probably depend on kinetic effects. Dipoles are the only possible equilibria for $\Upsilon < \Upsilon_m$, and for $\Gamma L < 0$ (with any value of Υ). For $\Gamma L > 0$ and $\Upsilon > \Upsilon_M$, there is no possible equilibrium. An additional constraint (3.34) expresses that the area of the equilibrium structure must be larger than the initial unmixed patch. This further reduces the possibility of equilibrium states, especially when Γ is small. For instance if $\Gamma = 0$, we get a translating dipole with radius a given by (3.32), and this is clearly excluded if the impulse P is too small. In that case, we expect the system to organize into two dipoles with opposite motion, so that each dipole can have a large proper impulse, although the total impulse is weak.

Of course these predictions rely on the linearized approximation, and we may wonder about its relevance for any given initial condition. A numerical resolution of the general variational problem would be then most useful, and the present analysis of the linearized case would provide a good guide to such an undertaking. This question

can also be addressed by expanding the results to higher orders in the argument $\beta\sigma\psi'$, as discussed by Chavanis & Sommeria (1996) in a bounded domain. This expansion involves the successive moments of vorticity (> 2), so new control parameters are introduced (e.g. the kurtosis), which makes the classification more complex. In a bounded domain, the linearized approximation turns out to be often reasonably good when both positive and negative vorticity can mix, which corresponds here to dipoles. Dipoles are indeed often observed with a relationship between vorticity and stream function which is not too far from linear (see e.g. Nguyen Duc & Sommeria 1988). Notice also that remarkably monopoles with a linear relationship have been observed in electron plasmas (Huang & Driscoll 1994), but we do not expect this feature to be general.

Self-organization into isolated vorticity structures is often observed in a fully turbulent field. Then it is not possible to clearly identify an initial condition with an isolated vorticity patch, from which we could calculate our integral constraints. Understanding the process of initial isolation is then a quite difficult problem which was not addressed here. However our approach could be useful to predict the result of vortex interactions once they are already well isolated from the background. It also provides general 'robustness' criteria for isolated vorticity structures.

This work was supported by the research program PATOM of the C.N.R.S. We have benefited from many discussions with R. Robert and the team of Laboratoire d'Analyse Numérique at Université de Lyon.

Appendix A. Relations between Lagrange multipliers and conserved quantities

We first prove the general relation (2.26) between the Lagrange multipliers and the conserved quantities. The conservation of the impulse results from the identity

$$\int \bar{\omega} u_x d^2 r_o = 0 \quad (\text{A } 1)$$

obtained by expressing u_x in terms of $\bar{\omega}$ by the Biot & Savart formula, and using antisymmetry arguments in the resulting integral (see e.g. Batchelor 1967, p. 528). With an integration by parts, (A 1) can be written

$$\int_{\mathcal{D}} x_o \mathbf{u} \nabla \bar{\omega} d^2 r_o = \oint x_o \bar{\omega} (\mathbf{u} \cdot \mathbf{i}_\zeta) d\chi \quad (\text{A } 2)$$

where the surface integral is restricted to the subdomain (\mathcal{D}), and the contour integral is along the boundary ($\partial\mathcal{D}$).

The relation between the absolute and the relative velocity corresponding to (2.16) is

$$\mathbf{u} = \mathbf{u}' + \boldsymbol{\Omega} \wedge \mathbf{r}_o + \mathbf{V}. \quad (\text{A } 3)$$

Using the condition $\mathbf{u}' \cdot \mathbf{i}_\zeta = \partial\psi'/\partial\chi = 0$ on the boundary (for a stationary state), we obtain

$$\int_{\mathcal{D}} x_o \mathbf{u} \nabla \bar{\omega} d^2 r_o = \oint x_o \bar{\omega} (\boldsymbol{\Omega} \wedge \mathbf{r}_o + \mathbf{V}) \mathbf{i}_\zeta d\chi. \quad (\text{A } 4)$$

Inside the subdomain, the vorticity and the stream function are connected by a relationship $\bar{\omega} = f_{\beta,g}(\psi')$. This implies $\mathbf{u}' \nabla \bar{\omega} = (-\mathbf{i}_z \wedge \nabla \psi') f'_{\beta,g}(\psi') \nabla \psi' = 0$ and there

remains

$$\mathbf{u}\nabla\bar{\omega} = (\boldsymbol{\Omega} \wedge \mathbf{r}_o + \mathbf{V})\nabla\bar{\omega}. \quad (\text{A } 5)$$

This relation expresses the link between the time derivative $\mathbf{u}\nabla\bar{\omega} = -\partial\bar{\omega}/\partial t$ and the space derivative for a structure in steady motion. Combining (A 4) and (A 5), we have

$$\int_{\mathcal{D}} x_o(\boldsymbol{\Omega} \wedge \mathbf{r}_o + \mathbf{V})\nabla\bar{\omega}d^2\mathbf{r}_o = \oint x_o\bar{\omega}(\boldsymbol{\Omega} \wedge \mathbf{r}_o + \mathbf{V})\mathbf{i}_\zeta d\chi \quad (\text{A } 6)$$

which is equivalent, with an integration by parts, to

$$\int_{\mathcal{D}} \bar{\omega}(V_x - \Omega y_o)d^2\mathbf{r}_o = 0 \quad (\text{A } 7)$$

that is to say $\Omega P_x = \Gamma V_x$. To prove (2.26), we need just to apply the same derivation to the y -component.

We now consider the case of a purely translating structure ($\Omega = \Gamma = 0$) and prove the relation (2.27) between its impulse and velocity. With an integration by parts, the impulse (2.8) can be written

$$P_x = \int_{\mathcal{D}} u_x d^2\mathbf{r}_o + \oint y_o(\mathbf{u} \cdot \mathbf{i}_\zeta) d\chi. \quad (\text{A } 8)$$

Since $u_x = \partial\psi/\partial y_o$, the first integral is equal to

$$\int_{\mathcal{D}} u_x d^2\mathbf{r}_o = \int [\psi(x_o, y_+(x_o)) - \psi(x_o, y_-(x_o))] dx_o \quad (\text{A } 9)$$

where $y_+(x_o)$ and $y_-(x_o)$ delimit the upper and lower boundaries of the subdomain (\mathcal{D}) in Cartesian coordinates. Now, for a purely translating motion at velocity V , we have $\psi = Vy - B$ on ($\partial\mathcal{D}$) so that

$$\int_{\mathcal{D}} u_x d^2\mathbf{r}_o = V \int [y_+(x_o) - y_-(x_o)] dx_o = V|\mathcal{D}|. \quad (\text{A } 10)$$

The impulse (A 8) can then be written

$$P_x = V|\mathcal{D}| + \oint y_o(\mathbf{u} \cdot \mathbf{i}_\zeta) d\chi. \quad (\text{A } 11)$$

The velocity field \mathbf{u} outside (\mathcal{D}) (and on the boundary) corresponds to the irrotational flow of an incompressible fluid due to a rigid body in translational motion V . Therefore, it must be of the form $\mathbf{u} = V\mathbf{u}_1$, where \mathbf{u}_1 is independent of V and depends only on position in the fluid relative to the body (see Batchelor 1967, p. 129). As a result, $P_x = C_{\mathcal{D}}|\mathcal{D}|V$ where

$$C_{\mathcal{D}} = 1 + \frac{1}{|\mathcal{D}|} \oint y_o(\mathbf{u}_1 \cdot \mathbf{i}_\zeta) d\chi \quad (\text{A } 12)$$

depends only on the domain (\mathcal{D}).

Appendix B. Second-order variations of the free energy in the linearized limit

In this Appendix, we show that the perturbations (3.39) and (3.45) can be associated with an incompressible velocity field of deformation (the conditions (i) and (ii) of §2.5 are satisfied) which does not change the constraints to first order. We also give

the main steps for solving the problem (2.46) and calculate the second variations of the free energy $\delta^2 J_d$.

In the case of monopoles, the relative velocity \mathbf{u}' vanishes only at the centre of the vortex (where the relative stream function is extremal). The perturbation (3.39) is also zero at this point in such a way that λ/u' remains finite. As a result, condition (i) is satisfied. Condition (ii) is also satisfied, as we can see by symmetry arguments: on each side of an axis $\lambda = 0$, the relative velocity u' is the same, but the perturbation λ has an opposite sign (with equal amplitude); therefore, the total integral (2.58) along a streamline $\psi' = \text{const.}$ is zero. As a result, there exists a velocity field \mathbf{U} satisfying $\nabla \cdot (\overline{\omega} \mathbf{U}) = \lambda$ and $\nabla \cdot \mathbf{U} = 0$. In fact, in the present case, we can obtain this velocity field explicitly. Indeed, using polar coordinates, (2.50) reduces to

$$U_r \frac{\partial \overline{\omega}}{\partial r} = \lambda(r, \theta) \quad (\text{B } 1)$$

since $\overline{\omega}(r)$ is purely axisymmetric. Then, with the aid of (3.11), we find

$$U_r(r, \theta) = -\frac{2\pi a^3 J_1(\alpha) J_m(kr)}{\Gamma' \alpha^2 J_1(kr)} \sin(m\theta) \quad (\text{B } 2)$$

and U_θ results from the incompressibility condition. We must check also that the deformation (3.39) satisfies the first-order constraints (2.52) and (2.53). Using polar coordinates, they can be rewritten

$$\delta L = \int_0^{2\pi} \overline{\omega}(a) U_r(a, \theta) a^3 d\theta - \int_0^a \int_0^{2\pi} r^3 \lambda(r, \theta) dr d\theta = 0, \quad (\text{B } 3)$$

$$\delta P_x = \int_0^{2\pi} \overline{\omega}(a) U_r(a, \theta) a^2 \sin \theta d\theta - \int_0^a \int_0^{2\pi} r^2 \sin \theta \lambda(r, \theta) dr d\theta = 0, \quad (\text{B } 4)$$

$$\delta P_y = -\int_0^{2\pi} \overline{\omega}(a) U_r(a, \theta) a^2 \cos \theta d\theta + \int_0^a \int_0^{2\pi} r^2 \cos \theta \lambda(r, \theta) dr d\theta = 0, \quad (\text{B } 5)$$

and are effectively satisfied when $m > 1$. We can now solve the problem (2.46) to determine the stream function Ψ . The result is

$$\Psi = -\frac{\lambda}{k^2} + K_m r^m \sin(m\theta) \quad (\text{B } 6)$$

where

$$K_m = \frac{1}{2m\alpha a^{m-2}} \left(J_{m-1}(\alpha) - \frac{2\pi a^2}{\Gamma' \alpha} J_m(\alpha) \overline{\omega}(a) \right). \quad (\text{B } 7)$$

In the linearized limit, we have $h'(\overline{\omega}) = 1/k^2$ and the expression (2.51) for the second variations of the free energy can be easily calculated yielding (3.41).

In the case of a dipole (3.16), the relative velocity \mathbf{u}' vanishes at the centre of each lobe and at the intersection of the separatrix and the edge of the vortex (this corresponds to the points with coordinates $r = a$, $\theta = 0, \pi$). The perturbation (3.45) is also zero at these points in such a way that λ/u' remains finite, as demanded by condition (i). On the other hand, symmetry arguments (with respect to the y -axis) similar to those used for the monopoles show that condition (ii) is also fulfilled. Finally, we can verify that the deformation (3.45) satisfies the first-order constraints

(2.52), (2.53) if we take

$$\eta = -\bar{\omega}(a) \frac{2\pi a^3 J_4(\alpha_{11})}{P'\alpha_{11} J_2(\alpha_{11})}. \quad (\text{B } 8)$$

The solution of problem (2.46) is therefore

$$\Psi = -\frac{\lambda}{k_{11}^2} - \frac{\eta}{6a\alpha_{11}} J_0(\alpha_{11}) r^3 \cos 3\theta + \frac{J_3(\alpha_{11})}{8a^2\alpha_{11}} r^4 \sin 4\theta. \quad (\text{B } 9)$$

With this expression, we can perform the integrals in (2.51) and obtain (3.47).

Appendix C. Generalization of Leith's results

In this Appendix, we generalize the results of Leith (1984) for any values of the control parameters E , Γ , L . We then recover his MEV M and MEV C solutions as particular cases. Finally, we point out that these solutions do not correspond to a minimum enstrophy state when we vary the radius, but rather to an inflection point.

Following Leith, we assume that the vorticity is confined to a circular subdomain (\mathcal{D}) of radius a , and we seek the axisymmetric (monopole) structure which has the minimum enstrophy:

$$G = \int \frac{1}{2} \omega^2 d^2\mathbf{r} \quad (\text{C } 1)$$

with the integral constraints

$$\Gamma = \int \omega d^2\mathbf{r}, \quad (\text{C } 2)$$

$$E = \int \frac{1}{2} \omega \psi_* d^2\mathbf{r} - \frac{\Gamma^2}{4\pi} \ln a \quad (\text{with } \psi_*(a) = 0), \quad (\text{C } 3)$$

$$L = \int \omega r^2 d^2\mathbf{r}. \quad (\text{C } 4)$$

In order to have a simpler boundary condition, we have redefined the stream function in (C 3) as $\psi_* \equiv \psi - \psi(a)$ (where $\psi(a) = -(\Gamma/4\pi) \ln a$ is obtained by solving the Laplace equation outside the vortex). Now, we want G to be a minimum with respect to variations in the vorticity field (at fixed radius) but also when we change the radius. Following Leith, we introduce a 'scaling' in order to separate these two kinds of variations. We set

$$s = r/a, \quad (\text{C } 5)$$

$$\omega(r) = \frac{\Gamma}{2\pi a^2} \hat{\omega}(s), \quad (\text{C } 6)$$

$$\psi_*(r) = \frac{\Gamma}{2\pi} \hat{\psi}_*(s). \quad (\text{C } 7)$$

The problem now consists in minimizing the enstrophy

$$\hat{G}(a, \hat{\omega}) \equiv \frac{4\pi G}{\Gamma^2} = \frac{1}{a^2} \int_0^1 \hat{\omega}^2 s ds \quad (\text{C } 8)$$

(considered as a function of the normalized vorticity field $\hat{\omega}$ and radius a) under the constraints

$$\int_0^1 \hat{\omega} s ds = 1, \quad (\text{C } 9)$$

$$\widehat{E} \equiv \frac{4\pi E}{\Gamma^2} = \int_0^1 \widehat{\omega} \widehat{\psi}_* s ds - \ln a \quad (\text{with } \widehat{\psi}_*(a) = 0), \quad (\text{C } 10)$$

$$\widehat{L} \equiv \frac{L}{\Gamma} = a^2 \int_0^1 \widehat{\omega} s^3 ds. \quad (\text{C } 11)$$

The corresponding variational principle can be written with Lagrange multipliers as

$$\delta \widehat{G} - \lambda \delta \widehat{E} - \gamma \delta \widehat{L} - \alpha \delta \Gamma = 0. \quad (\text{C } 12)$$

The variations over the vorticity field imply

$$\omega = \lambda \psi_* + \frac{\gamma \Gamma}{4\pi} r^2 + \frac{\alpha \Gamma}{4\pi} \quad (\text{C } 13)$$

and the variations over the radius yield

$$G = \frac{\Gamma^2}{8\pi} \lambda - \frac{\Gamma L}{4\pi} \gamma. \quad (\text{C } 14)$$

The first equation is identical to (3.1) with slightly different notation. Now, Leith determines the optimal radius by the condition (C 14) which cancels the first variations of the enstrophy versus radius. We can show after a tedious calculation that (C 14) is equivalent to having $\omega(a) = 0$. Therefore, the monopole settles its radius so as to avoid any discontinuity at the boundary. As a result, Leith's minimum enstrophy vortices are characterized by a continuous vorticity and a linear relationship $\omega = f(\psi')$. We have reached the same conclusions in the framework of the maximum entropy bubble but for different reasons. Accordingly, a generalization of Leith theory (for any values of the control parameters) leads to the same equation of state as (3.24), (3.25).

At this stage, it is interesting to recover the two particular cases considered by Leith:

(i) MEV M: when $\Gamma \rightarrow 0$, the control parameter reduces to $Y \sim 4\pi E/\Gamma^2 \rightarrow +\infty$ and the monopole temperature determined by (3.25) is simply $\alpha = \alpha_{2m}$. In this limit, equations (3.24), (3.25) are equivalent to

$$\frac{L}{\Gamma a^2} \sim -\frac{J_3(\alpha)}{\alpha J_2(\alpha)} \quad \text{and} \quad Y \sim \frac{3J_3^2(\alpha)}{\alpha^2 J_2^2(\alpha)}.$$

The radius of the MEV M monopole is therefore

$$a = \left(\frac{3L^2}{4\pi E} \right)^{1/4} \quad (\text{C } 15)$$

as found by Leith.

(ii) MEV C: when $\Omega = 0$ (i.e the constraint on the angular momentum is released), the formula (3.12) with $\Gamma' = \Gamma$, combined with (3.24) yields $\alpha = \alpha_{0m}$. We find with the equation of state (3.25) that these solutions correspond to control parameters:

$$Y = \frac{1}{2} + \frac{1}{2} \ln \left(1 - \frac{4}{\alpha_{0m}^2} \right). \quad (\text{C } 16)$$

The radii of the MEV C monopoles, determined by (3.24), are

$$\frac{L}{\Gamma a^2} = 1 - \frac{4}{\alpha_{0m}^2} \quad (\text{C } 17)$$

or equivalently:

$$E = \frac{\Gamma^2}{4\pi} \left(\frac{1}{2} - \ln a \right) \quad (\text{C } 18)$$

without reference to the angular momentum.

However, these solutions only cancel the first variations of the enstrophy. Their stability will depend on the second-order variations. For a given radius, the monopole with zero circulation (MEV M) is stable under axisymmetric perturbations but not under quadripolar perturbations (since $\alpha_{2m} > \alpha_{11}$) as discussed in § 3.4 (our conditions of stability apply also to minimum-enstrophy vortices, as discussed at the end of § 4). For the same reason, only the MEV C with $m = 1$ (corresponding to $\Upsilon \simeq -0.08828$) is stable. Therefore, non-axisymmetric perturbations (which Leith did not consider) are more destabilizing than axisymmetric ones and must be taken into account in the stability problem.

Leith examined also the second variations of the enstrophy with respect to radius changes and showed that they were positive. In order to have a true minimum, they must in fact be strictly positive. Now, the enstrophy of a linear monopole with radius a is

$$G = \frac{\Gamma^2}{4\pi a^2} \left\{ 2 + \alpha^2 \mathcal{H} \left(1 + \frac{A^2 J_1(\alpha)}{3 J_3(\alpha)} \right) \right\} \quad (\text{C } 19)$$

with the notation of § 3.2. According to (3.13)–(3.15), the normalized enstrophy $(4\pi L/\Gamma^3)G$ is a function of Υ and $L/\Gamma a^2$ only. In particular, for a given control parameter Υ , we can plot the enstrophy as a function of $a|\Gamma/L|^{1/2}$ (see figure 7). We then observe that the enstrophy is always decreasing and that the monopole with a continuous vorticity corresponds to an inflection point and not to an enstrophy minimum. In contrast, our criterion of boundary deformation indicates that this particular monopole is stable.

REFERENCES

- BATCHELOR, G. K. 1967 *An Introduction to Fluid Dynamics*. Cambridge University Press.
- CARTON, X., FLIERL, G. R. & POLVANI, L. M. 1989 The generation of tripoles from unstable axisymmetric isolated vortex structures. *Europhys. Lett.* **9**, 339–344.
- CARTON, X. & LEGRAS, B. 1994 The life-cycle of tripoles in two-dimensional incompressible flows. *J. Fluid Mech.* **267**, 53–82.
- CHAPLYGIN, S. A. 1902 One case of vortex motion in fluid. *Proc. Phys. Sec. Nat. Phil. Soc.* **11**, 114.
- CHAVANIS, P. H. & SOMMERIA, J. 1996 Classification of self-organized vortices in two-dimensional turbulence: the case of a bounded domain. *J. Fluid Mech.* **314**, 267–297.
- CHAVANIS, P. H., SOMMERIA, J. & ROBERT, R. 1996 Statistical mechanics of two-dimensional vortices and collisionless stellar systems. *Astrophys. J.* **471**, 385–399.
- CHORIN, A. J. 1994 *Vorticity and Turbulence*. Springer.
- COUDER, Y. & BASDEVANT, C. 1986 Experimental and numerical study of vortex couples in two dimensional flows. *J. Fluid Mech.* **173**, 225–251.
- FLIERL, G. R. 1987 Isolated eddy models in geophysics. *Ann. Rev. Fluid Mech.* **19**, 493–530.
- FLIERL, G. R., STERN, M. E. & WHITEHEAD, J. A. 1983 The physical significance of modons: laboratory experiments and general integral constraints. *Dyn. Atmos. Oceans* **7**, 233–263.
- HEIJST, G. J. F. VAN & FLOR, J. B. 1989 Dipole formation and collisions in a stratified fluid. *Nature* **340**, 212–215.
- HEIJST, G. J. F. VAN, KLOOSTERZIEL, R. C. & WILLIAMS, C. W. M. 1991 Laboratory experiments on the tripolar vortex in a rotating fluid. *J. Fluid Mech.* **225**, 301–331.
- HJORTH, J. & MADSEN, J. 1991 Violent relaxation and the $R^{1/4}$ law. *Mon. Not. R. Astron. Soc.* **253**, 703–709.

- HUANG, X. P. & DRISCOLL, C. F. 1994 Relaxation of 2D turbulence to a metaequilibrium near the minimum enstrophy state. *Phys. Rev. Lett.* **72**, 2187–2190.
- JOYCE, G. & MONTGOMERY, D. 1973 Negative temperature states for the two-dimensional guiding-centre plasma. *J. Plasma Phys.* **10**, 107–121.
- KLOOSTERZIEL, R. C. & HEIJST, G. J. F. VAN 1991 An experimental study of unstable barotropic vortices in a rotating fluid. *J. Fluid Mech.* **223**, 1–24.
- KLOOSTERZIEL, R. C. & HEIJST, G. J. F. VAN 1992 The evolution of stable barotropic vortices in a rotating free-surface fluid. *J. Fluid Mech.* **239**, 607–629.
- KRAICHNAN, R. H. & MONTGOMERY, D. 1980 Two-dimensional turbulence. *Rep. Prog. Phys.* **43**, 547–617.
- KUZ'MIN, G. A. 1982 Statistical mechanics of the organisation into two-dimensional coherent structures. In *Structural Turbulence* (ed. M. A. Goldshtik), pp. 103–114. Acad. Nauk CCCP Novosibirsk, Institute of Thermophysics.
- LAMB, H. 1932 *Hydrodynamics*, 6th edn. Dover.
- LEGRAS, B., SANTANGELO, P. & BENZI, R. 1988 High resolution numerical experiments for forced two-dimensional turbulence. *Europhys. Lett.* **5**, 37–42.
- LEITH, C. E. 1984 Minimum enstrophy vortices. *Phys. Fluids* **27**, 1388–1395.
- LUNDGREN, T. S. & POINTIN, Y. B. 1977 Statistical mechanics of two-dimensional vortices. *J. Statist. Phys.* **17**, 323–355.
- LYNDEN-BELL, D. 1967 Statistical mechanics of violent relaxation in stellar systems. *Mon. Not. R. Astron. Soc.* **136**, 101–121.
- MCWILLIAMS, 1984 The emergence of isolated coherent vortices in turbulent flow. *J. Fluid Mech.* **146**, 21–43.
- MELESHKO, V. V. & VAN HEIJST, G. J. F. 1994 On Chaplygin's investigations of two-dimensional vortex structures in an inviscid fluid. *J. Fluid Mech.* **272**, 157–182.
- MILLER, J. 1990 Statistical mechanics of Euler equations in two dimensions. *Phys. Rev. Lett.* **65**, 2137–2140.
- MONTGOMERY, D., MATTHAEUS, W., STRIBLING, W., MARTINEZ, D. & OUGHTON, S. 1992 Relaxation in two dimensions and the sinh-Poisson equation. *Phys. Fluids A* **4**, 3–6.
- NGUYEN DUC, J. M. & SOMMERIA, J. 1988 Experimental characterization of steady two-dimensional vortex couples. *J. Fluid Mech.* **192**, 175–192.
- ONSAGER, L. 1949 Statistical hydrodynamics. *Nuovo Cimento Suppl.* **6**, 279–287.
- PASMANTER, R. A. 1994 On long lived vortices in 2D viscous flows, most probable states of inviscid 2D flows and a soliton equation. *Phys. Fluids* **6**, 1236–1241.
- ROBERT, R. 1990 Etats d'équilibre statistique pour l'écoulement bidimensionnel d'un fluide parfait. *C. R. Acad. Sci. Paris I* **311**, 575–578.
- ROBERT, R. 1991 Maximum entropy principle for two-dimensional Euler equations. *J. Statist. Phys.* **65**, 531–551.
- ROBERT, R. & ROSIER, 1997 The modelling of small scales in 2D turbulent flows: a statistical mechanical approach. *J. Statist. Phys.* **86**, 481–515.
- ROBERT, R. & SOMMERIA, J. 1991 Statistical equilibrium states for two-dimensional flows. *J. Fluid Mech.* **229**, 291–310.
- SOMMERIA, J. 1994 Organized vortices as maximum entropy structures. In *Modelling of Oceanic Vortices* (ed. G. J. F. van Heijst), pp. 37–50. North-Holland.
- SOMMERIA, J., STAQUET, C. & ROBERT, R. 1991 Final equilibrium state of a two dimensional shear layer. *J. Fluid Mech.* **233**, 661–689.
- STERN, M. 1975 Minimal properties of planetary eddies. *J. Mar. Res.* **33**, 1–13.
- WHITAKER, N. & TURKINGTON, B. 1994 Maximum entropy states for rotating vortex patches. *Phys. Fluids* **6**, 3963–3973.